BRNO UNIVERSITY OF TECHNOLOGY

VYSOKÉ UČENÍ TECHNICKÉ V BRNĚ

CENTRAL EUROPEAN INSTITUTE OF TECHNOLOGY BUT

STŘEDOEVROPSKÝ TECHNOLOGICKÝ INSTITUT VUT

DEVELOPMENT OF FOURIER TRANSFORM INFRARED SPECTROSCOPY IN HIGH MAGNETIC FIELDS

VÝVOJ INFRAČERVENÉ SPEKTROSKOPIE S FOURIEROVOU TRANSFORMACÍ V SILNÝCH MAGNETICKÝCH POLÍCH

SHORT VERSION OF DOCTORAL THESIS

TEZE DIZERTAČNÍ PRÁCE

AUTHOR
AUTOR PRÁCE
Ing. Jana Dubnická Midlíková

SUPERVISOR
ŠKOLITEL
doc. Ing. Petr Neugebauer, Ph.D.

CO-SUPERVISOR
ŠKOLITEL SPECIALISTA
doc. Mgr. Adam Dubroka, Ph.D.

BRNO 2023

Abstract

Fourier-transform infrared (FTIR) spectroscopy in high magnetic fields, concisely FTIR magneto-spectroscopy, is a powerful spectroscopic technique used to investigate many important effects in materials, e.g., electron paramagnetic resonance, cyclotron resonance, and transitions between Landau levels. Despite their enormous potential in solid-state physics, infrared magneto-spectrometers are still relatively rare and custom-made since such systems generally require complex infrastructure. This doctoral thesis describes in detail the design and implementation of a versatile FTIR magneto-spectroscopic setup operating in the range of 50–10,000 cm^{-1}, high magnetic field up to 16 T and temperatures between 2–320 K located at the Central European Institute of Technology of Brno University of Technology. This setup allows us to perform a variety of magneto-optical measurements spanning the range from THz/far-infrared (FIR) to near-infrared (NIR). It consists of a commercial FTIR spectrometer coupled to a 16 T cryogen-free superconductive magnet by the custom-designed optical coupling and transmission probes designed for experiments with multiple detectors and samples in Faraday geometry. The novelty of the setup lies in the usage of a cryogen-free superconducting magnet. We have optimized and tested the performance of the FTIR magneto-spectroscopic setup for various configurations and determined a workable setup range. The functionality of the FTIR magneto-spectroscopic setup was demonstrated by the magneto-optical measurements of the zero-field splitting in cobalt(II)-based single ion magnet in the FIR region, indirect inter-band transitions between Landau levels (LLs) in germanium in the NIR region, and inter-band transitions between LLs in graphene in the FIR region. Moreover, we measured the I-V characteristics of graphene bolometer devices.

Keywords

Fourier-transform infrared (FTIR) magneto-spectroscopy, FTIR magneto-spectroscopic setup, cryogen-free superconducting magnet, single molecule magnets, electron paramagnetic resonance, Landau levels

Abstrakt

Infračervená spektroskopie s Fourierovou transformací (FTIR) v silných magnetických polích, zkráceně FTIR magnetospektroskopie, je výkonná spektroskopická technika používaná ke zkoumání mnoha důležitých jevů v materiálech, např. elektronové paramagnetické rezonance, cyklotronové rezonance a přechodů mezi Landauovými hladinami. Navzdory svému obrovskému potenciálu ve fyzice pevných látek jsou infračervené magnetospektrometry stále poměrně vzácné a vyráběné na zakázku, protože takové systémy obvykle vyžadují složitou infrastrukturu. Tato disertační práce podrobně popisuje návrh a realizaci univerzálního FTIR magnetospektroskopického zařízení pracujícího v rozsahu 50–10 000 cm^{-1}, silném magnetickém poli až 16 T a teplotách mezi 2–320 K umístěné na Středoevropském technologickém institutu VUT v Brně. Toto zařízení nám umožňuje provádět různá magnetooptická měření v rozsahu od THz/vzdálené infračervené oblasti (FIR) až po blízkou infračervenou oblast (NIR). Skládá se z komerčního FTIR spektrometru spojeného s 16 T bezkryogenním supravodivým magnetem pomocí na míru navržené optické spojky a přenosových sond určených pro experimenty s více detektory a vzorky ve Faradayově geometrii. Novinka tohoto uspořádání spočívá v použití supravodivého magnetu bez kryogenu. Optimalizovali jsme a otestovali výkonnost FTIR magnetospektroskopického zařízení pro různé konfigurace a určili použitelný rozsah zařízení. Funkčnost FTIR magnetospektroskopického zařízení byla prokázána magnetooptickými měřeními štěpení při nulovém poli v jednoiontovém magnetu na bázi kobaltu(II) v oblasti FIR, nepřímých mezipásmových přechodů mezi Landauovými hladinami (LLs) v germániu v NIR oblasti a mezipásmových přechodů mezi LLs v grafenu v oblasti FIR. Kromě toho jsme změřili volt-ampérové charakteristiky grafenových bolometrických zařízení.

Klíčová slova

infračervená magnetospektroskopie s Fourierovou transformací (FTIR), FTIR magnetospektroskopické zařízení, supravodivý magnet bez kryogenu, jednomolekulové magnety, elektronová paramagnetická rezonance, Landauovy hladiny

DUBNICKÁ MIDLÍKOVÁ, Jana. *Development of Fourier Transform InfraRed Spectroscopy in High Magnetic Fields*. Short version of doctoral thesis. BUT CEITEC: Brno University of Technology, Central European Institute of Technology, Brno, 2023. 48 p. Supervised by doc. Ing. Petr Neugebauer, Ph.D.

Declaration

I hereby declare that I have elaborated my doctoral thesis on the theme of "Development of Fourier Transform InfraRed Spectroscopy in High Magnetic Fields" independently, under the supervision of doc. Ing. Petr Neugebauer, Ph.D., co-supervisor doc. Mgr. Adam Dubroka, Ph.D., and with the use of literature and other sources of information, which are all quoted in the thesis and detailed in the References at the end of this thesis.

Ing. Jana Dubnická Midlíková

Acknowledgement

I want to thank all those who contributed directly or indirectly to this work. First of all, I would like to thank my supervisor, doc. Ing. Petr Neugebauer, Ph.D., and co-supervisor doc. Mgr. Adam Dubroka, Ph.D. for professional guidance and consultations. I want to thank all members of our CEITEC MOTeS research group for useful discussions and comments during the development of the setup and friendly environment, namely Dr. Vinicius Santana for his tremendous willingness and help with the analysis of data, Ing. Antonín Sojka, PhD., Ing. Matúš Šedivý, Dr. Oleksii Laguta, for their helpful advice with mechanical design, the electronics, and the laboratory equipment, and doc. Ing. Ivan Šalitroš, Ph.D. and Ing. Jana Juráková for providing samples. Then, I would like to thank Dominik Varga (CEITEC Nano research infrastructure, Brno, Czech Republic) for the fabrication of the setup components in the mechanical workshop. I would also like to thank RNDr. Milan Orlita, Ph.D. (Grenoble High Magnetic Field Laboratory, Grenoble, France) for helpful advice during the design and optimization of the setup and fruitful discussions over the results of magneto-optical measurements and Ing. Aleš Srnka, CSc. (Institute of Scientific Instruments of the Czech Academy of Sciences, Brno, Czech Republic) for help in the organization of measurements. Special thanks belong to my beloved husband, Ladislav, and my family for their love, encouragement, and constant support.

My work and research has been financially supported by the European Research Council (ERC) through the European Union's Horizon 2020 Research and Innovation Program under Grant 714850, Ministry of Education, Youth and Sports of the Czech Republic (MEYS CR) under the INTER-EXCELLENCE Program under Grant LTAUSA19060. Moreover, I was supported by Brno Ph.D. Talent 2018 scholarship by JCMM and by Internal junior grant project within CEITEC BUT 2019. This research has been also financially supported by the MEYS CR under the project CEITEC 2020 (LQ1601) and part of the work was carried out with the support of CEITEC Nano Research Infrastructure (ID LM2015041, MEYS CR, 2016-2019), CEITEC Brno University of Technology. CzechNanoLab project LM2018110 and LM2023051, funded by MEYS CR, is gratefully acknowledged for the measurements at CEITEC Nano Research Infrastructure.

Ing. Jana Dubnická Midlíková

Contents

Introduction

This doctoral thesis deals with Fourier-transform infrared (FTIR) spectroscopy in high magnetic fields, concisely FTIR magneto-spectroscopy, a powerful spectroscopic technique used to investigate many important effects in materials, e.g., electron paramagnetic resonance (EPR), cyclotron resonance, and transitions between Landau levels (LLs). In the thesis, we describe the design and implementation of a versatile broadband setup for FTIR magneto-spectroscopy operating in the range of 50–10,000 cm^{-1}, high magnetic field up to 16 T and temperatures between 2–320 K located at the Central European Institute of Technology of Brno University of Technology (CEITEC BUT). This setup allows us to perform a variety of magneto-optical measurements spanning the range from THz/far-infrared (FIR) to near-infrared (NIR). FTIR magneto-spectroscopic setup consists of a commercial FTIR spectrometer and 16 T cryogen-free superconducting magnet coupled with custom-designed optical coupling and transmission probes for experiments performed on various samples in Faraday geometry using multiple detectors with two possibilities of their placement, outside and inside the superconducting magnet. Using various detectors, the setup spans the entire IR and partially the THz range. This aspect is particularly important because it enables the measurement of different types of samples from single molecule magnets (SMMs) in the FIR region to germanium in the NIR region, as demonstrated in the magneto-optical measurements chapter. Another novelty of the setup lies in the usage of a cryogen-free superconducting magnet.

This doctoral thesis is divided into four chapters. The first chapter, entitled "Theoretical Background," provides a theoretical framework for understanding the key concepts and phenomena that underpin our research topic. It comprises sections about electromagnetic radiation, IR spectroscopy, and FTIR spectrometer. Last but not least, the importance of high magnetic fields is explained.

Spectroscopy is one of the most fundamental and widespread experimental techniques for scientific investigation. All types of spectroscopic techniques have one thing in common; they all study the interaction of electromagnetic radiation with matter. The interactions are characterized by the energy of the radiation and its effects on materials. When the radiation energy falls within the IR region of the electromagnetic spectrum, we speak of IR spectroscopy. IR spectroscopy is considered one of the most powerful and widespread spectroscopic tools of the 20th and 21st centuries [1]. It provides detailed information about molecular vibrations. The history of IR spectroscopy can be traced back to the work of Sir William Herschel, who in 1800 discovered IR radiation beyond the red end of the visible spectrum when he

investigated the heating effect of sunlight [2]. However, a major breakthrough in IR spectroscopy that led to its widespread use came in the 1970s with the introduction of Fourier-transform infrared (FTIR) spectrometers equipped with interferometers, exploiting the well-established mathematical process of Fourier transform (FT) [3]. Due to its significantly improved acquisition of IR spectra, leading to better signal-to-noise and reduced data acquisition time, the FTIR spectrometers are nowadays predominantly used spectrometers in the IR range [4]. Thus, IR spectroscopy is frequently referred to as FTIR spectroscopy.

The second chapter, entitled "FTIR magneto-spectroscopy," introduces the core technique of the doctoral thesis and explains the physical principles and effects underpinning our research, i.e., electron paramagnetic resonance (EPR) and transitions between Landau Levels (LLs). It also describes in detail the most relevant class of materials for our research, i.e., SMMs.

FTIR spectroscopy in high magnetic field or simply FTIR magneto-spectroscopy is a powerful spectroscopic technique used to investigate many important effects in materials, e.g., EPR, cyclotron resonance, and transitions between LLs [5, 6]. FTIR magneto-spectroscopy is an essential method in the characterization of SMMs, molecules displaying slow relaxation of magnetization of purely molecular origin [7], thus the ability to store one bit of information at much higher densities, due to the ability to probe molecular and electronic properties directly [8, 9]. It allows studying EPR phenomenon in SMMs with very large zero-field splitting (ZFS), mainly based on transition metal complexes [10] – [17] or lanthanides [18] – [21], in which conventional microwave EPR systems do not provide experimental access to the magnetic resonance transitions. Besides, FTIR magneto-spectroscopy also presents an ideal experimental technique that can investigate band structure and electronic properties of materials such as graphene [22] – [27]. However, despite their enormous potential in material science, IR magneto-spectrometers are still relatively rare and custom-made since such systems generally require complex infrastructure.

The third chapter, "Experimental Setup," is dedicated to the design and implementation of the home-build FTIR magneto-spectroscopic setup at CEITEC BUT. This chapter maps the process from the design of the setup to the summary of the setup's performance. It consists of sections about Beam propagation, Setup Design and Components, and Performance of the setup.

The last, fourth chapter of the thesis, entitled "Magneto-Optical Measurements," provides results obtained on our FTIR magneto-spectroscopic setup at CEITEC BUT. These results include the magneto-optical measurements by which the functionality of our setup was demonstrated, i.e., the ZFS in cobalt(II)-based single ion magnet in the FIR region, and indirect inter-band transitions between Landau levels (LLs) in germanium in the NIR region.

Aims of Thesis

The ultimate goal of my doctoral studies and this thesis is to realize the method of FTIR spectroscopy in high magnetic fields by the development of the compact FTIR magneto-spectroscopic setup at CEITEC BUT in order to perform sensitive magneto-optical measurements on SMMs, novel 2D materials, or combination of both. It consists of several minor aims that need to be carried out to accomplish the ultimate goal. Therefore, I formulate my aims as follow:

1. **Overall design of the FTIR magneto-spectroscopic setup**
   The first aim is focused on the overall design of the compact FTIR magneto-spectroscopic setup. This comprises mainly the design of the coupling of FTIR spectrometer superconducting magnet and external detectors. The coupling consists of two main parts: optical coupling, which guides the beam out of the spectrometer to the magnet, and two types of transmission probes/waveguides, which guide the beam through the sample placed in the magnet to the detector. The first probe A is designed to measure the sample/reference signal by the detector placed outside the superconducting magnet (e.g., room temperature detectors). The second probe B is designed for the detector placed inside the superconducting magnet (i.e., sealed bolometer) and for testing measurements on graphene bolometer devices incorporated in a chipset holder. This part also includes the design of a movable table on which FTIR spectrometer and part of the setup is placed.

2. **Assembly, testing and putting the setup into the operation**
   When the design and manufacture of individual components are completed, the setup will be assembled and put into operation. This includes testing, troubleshooting the setup, and optimizing its performance to prepare it for magneto-optical measurements properly. The first step to test the setup's performance will be measuring the signal that passes through the setup and the sample/reference to the DTGS or InGaAs detector without a magnetic field. If the signal at the detector is insufficient, we will look for ways to improve it. When the signal is sufficient, we will test the performance of the setup in all possible configurations of probes, detectors, sources, and beamsplitters with no sample, just reference opening, and without a magnetic field. Then, samples with already published results will be measured to provide a comparison of the obtained results. Upon successful completion of this part, the FTIR magneto-spectroscopic setup will be functional, and magneto-optical measurements of desired samples can be carried out.

3. **Performance of magneto-optical measurements at CEITEC BUT**
   The final aim is to perform magneto-optical measurements on the home-built FTIR magneto-spectroscopic setup at CEITEC BUT. This state-of-the-art instrumentation will be useful for revealing interesting properties of SMMs with very large zero-field splitting (promising molecules for future data storage and spintronics), novel 2D materials, and testing graphene bolometric devices. After recording a sufficient number of spectra, emphasis will be placed on careful analysis of experimentally measured data (theoretical simulations and fitting) and searching for results of scientific importance, which will then be summarized and published in peer-reviewed journals.

1 Theoretical Background

In this chapter, we will provide a theoretical background and overview of the fundamental concepts relevant to the topic of the doctoral thesis, i.e., Fourier Transform Infrared (FTIR) spectroscopy in high magnetic fields. This will include an introduction to electromagnetic radiation, infrared spectroscopy, FTIR spectrometer, and high magnetic fields.

1.1 Electromagnetic Radiation

Electromagnetic radiation can be described as the flow of electromagnetic energy through the space or material medium. It can be considered in terms of classical (wave) or quantum (particle) theories [1].

Electromagnetic radiation is, classically speaking, a wave composed of oscillating electric and magnetic fields, hence the term "electromagnetic", acting in planes that are perpendicular to each other and to the direction of propagation [28]. The magnitudes of the electric and magnetic vectors are represented by E and B, respectively. In vacuum, the propagation velocity of electromagnetic waves is constant for all frequencies, and it is known as the speed of light, denoted as c, and has the value c = 2.99792458 x $10^8\,\mathrm{m\,s^{-1}}$ [29]. The phase[1] velocity of electromagnetic waves varies with the refractive index n of the medium and it is given by c/n [1], [28] whereas frequency is independent of the medium in which it is measured.

Electromagnetic radiation/wave is usually characterized by its wavelength λ, which is the length of one wave, and its frequency ν, which is the number of vibrations per unit time, usually in units hertz (Hz) [30]. They are related to each other and to the speed of light c in the following way:

$$c = \lambda\nu. \tag{1.1}$$

Another unit to characterize electromagnetic waves, widely used in infrared spectroscopy, is called wavenumber, $\tilde{\nu}$, which represents the number of waves per unit length and is given by the following relationship:

$$\tilde{\nu} = 1/\lambda = \nu/c. \tag{1.2}$$

Wavenumber is usually expressed in units called reciprocal/inverse centimeters abbreviated as $\mathrm{cm^{-1}}$, but it could be expressed in any reciprocal distance units [3]. Using frequency and wavenumber units have two main advantages over wavelength units.

[1] The phase velocity of a wave is the rate at which the wave propagates in any medium.

The first is that they remain constant regardless of the medium through which the radiation passes, whereas the wavelength decreases if the radiation passes through a medium with a refractive index n greater than that of a vacuum. The second advantage is that they are directly proportional to the energy. Therefore, a transition that requires more energy will occur at a higher wavenumber. For this reason, wavenumber units are commonly used in IR spectroscopy as opposed to wavelength units (e.g., nanometers), which are commonly used in visible and ultraviolet (UV) spectroscopy [3].

In terms of modern quantum theory, electromagnetic radiation is the flow of photons (quanta) through space. Photons are uncharged massless elementary particles that move with the speed of ligh in vacuum, exhibit wave–particle duality[2] [31] and represent a quantum of the electromagnetic field [32]. In 1900, Max Planck[3] postulated the quantum hypothesis that the energy of a single photon is quantized, so that all material systems can absorb or emit electromagnetic radiation only in quanta of energy E, which are proportional to the frequency of this radiation ν, whose value is the same as that of the frequency of the electromagnetic wave of classical theory [1]. This relationship is given by Planck's equation

$$E = h\nu = hc\tilde{\nu}, \tag{1.3}$$

where $h\nu$ is a quantum of energy, and h is a universal constant which is known as Planck's constant, which has a value $h = 6.62606876 \text{ x } 10^{-34}\,\text{J s}$ [29]. A commonly used unit of energy is the electronvolt (eV) which is defined as the kinetic energy acquired by an electron which has been accelerated by a potential difference of 1 volt (V). The electronvolt is related to the more usual unit of energy by: $1 \text{ eV} = 1.60218 \text{ x } 10^{-19}\,\text{J}$ [29].

In 1913, Niels Bohr postulated that the electrons of an atom occupy specific energy states or levels (also called quantum states) that are defined by the radius of the electron's orbit around the nucleus. Atoms must absorb or emit energy equal to the energy difference between the two levels to move between different energy states, see Fig. 1.1. By moving from a higher energy state E_h to a lower energy state E_l, a photon of energy $h\nu$ (quantum of electromagnetic radiation), is emitted of a magnitude that is precisely the energy difference ΔE between the higher E_h and lower E_l state [3]:

$$\Delta E = E_h - E_l = h\nu. \tag{1.4}$$

Alternatively, the electron can absorb a photon $h\nu$ and move from E_l to E_h if $h\nu$ matches the energy difference [3].

[2] their behavior featuring properties of both waves and particles [31]

[3] In 1918, Max Planck was awarded the Nobel Prize in Physics for his work on quantum theory [33].

Each element has electrons at unique energy levels corresponding to its atomic structure. When an element is exposed to radiation of all wavelengths, only the wavelengths (energy photons) corresponding to that atom's levels (energy states) can interact. The resulting pattern of energy lines, called a spectrum, coincides with the absorption or emission of photons specific to that element [3].

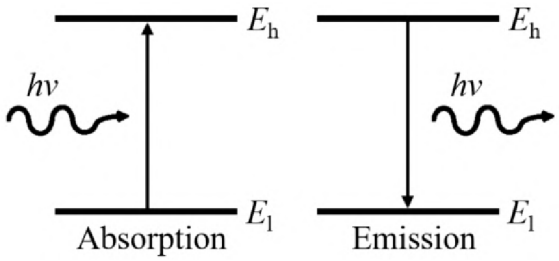

Fig. 1.1: The photon of energy $h\nu$ whose frequency matches the energy difference between electronic levels (higher energy state E_h and lower energy state E_l) can be absorbed or emitted as the electron transitions between the two levels. Adapted from [3].

The electromagnetic spectrum is the range of electromagnetic radiation distributed according to frequency, wavelength, or photon energy. In order of increasing frequency/energy and decreasing wavelength, it includes radio waves, microwaves (MWs), infrared (IR) radiation, visible light, ultraviolet (UV) radiation, X-rays and gamma-rays (γ-rays) [28]. These regions are illustrated in Fig. 1.2. There are no precise accepted boundaries between any of these adjacent regions of the electromagnetic spectrum, so the ranges usually overlap.

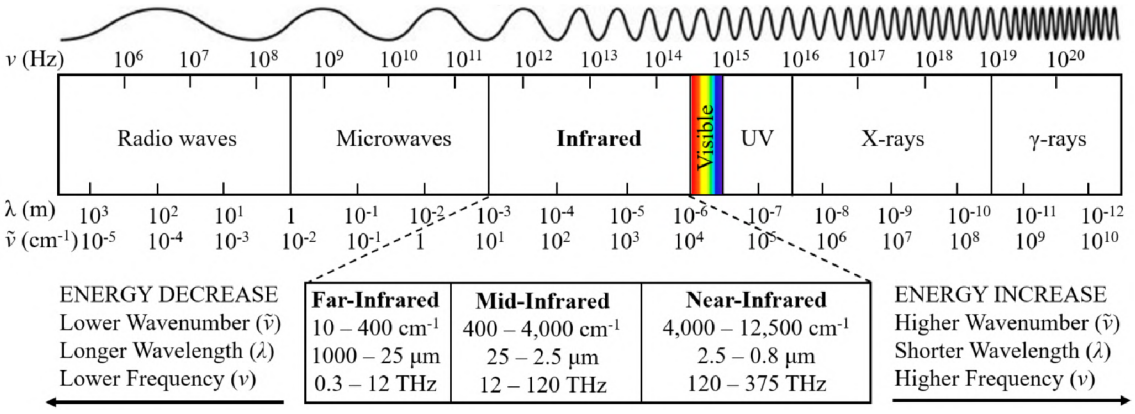

Fig. 1.2: The electromagnetic spectrum with expansion of the IR region.

Beyond the red end of the visible range but at frequencies higher than those of MWs, there is the IR region of the electromagnetic spectrum, discovered in

1800 by Sir William Herschel [2], roughly defined in the wavenumber[4] range 10–12,500 cm^{-1} (1 mm–800 nm, 1.24 meV–1.56 eV, 300 GHz–375 THz), which is rather broad in terms of energy; therefore, it is divided into three subregions: near-infrared (NIR) (4,000–12,500 cm^{-1}), mid-infrared (MIR) (400–4,000 cm^{-1}), and far-infrared (FIR) (10–400 cm^{-1}) [34], as illustrated in Fig. 1.2.

Between the MWs and the IR region, there is the terahertz (THz) region partially overlapping with the FIR region filling the frequency gap. It is usually defined as the region extending from 0.1 THz to 3 THz (3.3–100 cm^{-1}). For the last two decades, THz spectroscopy has developed remarkably due to its intriguing applications in solid-state physics, material science, physical and analytical chemistry, biomedicine [34] – [36]. The emergence of THz spectroscopy to some extent also represented the renaissance of the FIR region [37].

1.2 Infrared Spectroscopy

IR spectroscopy is based on the vibrations of the atoms of a molecule [28]. It is a versatile experimental technique based on the vibrations of the atoms of a molecule [28] providing detailed information about molecular vibrations, which are useful for identifying molecules, studying their structure, and interactions with a surrounding environment [1]. It is widely used in fields such as chemistry, biochemistry, and materials science and has applications in areas such as the pharmaceutical industry, forensics, biomaterials, food industry, paper and paint industry, environmental analysis, astronomy [38], etc. Therefore, it is no surprise that IR spectroscopy is considered one of the most powerful and widespread analytical spectroscopic tools of the 20th and 21st centuries [1].

1.3 FTIR Spectrometer

A major breakthrough in IR spectroscopy that led to its widespread use came in the 1970s with the introduction of FTIR spectrometers equipped with interferometers, exploiting the well-established mathematical process of Fourier transform(FT) [3]. Due to its significantly improved acquisition of IR spectra, leading to better SNR and reduced data acquisition time, the FTIR spectrometers are nowadays predominantly used spectrometers in the IR range [4]. Thus, IR spectroscopy is frequently referred to as FTIR spectroscopy.

FTIR spectrometer consists primarily of interferometer (usually Michelson-type), source of radiation, the detector and other optical elements (beamsplitters, mirrors,

[4]Energy unit conversion of 1 cm^{-1} = 10 mm ≅ 0.12 meV ≅ 30 GHz.

etc.). Then, it includes sample compartment, amplifier, analog-to-digital converter (ADC), and of course, computer, where experiment control, data acquisition and manipulation takes place. The radiation emitted by the source goes through the interferometer, passes through the sample and is then detected. The FTIR spectroscopy is based on the principle of interference of the radiation between two beams to obtain an interferogram – analog signal at the detector originated as a function of the path-length difference between the beams. The signal is amplified by amplifier, in which high-frequency components are filtered out. After that, the signal/interferogram is converted to digital form by an ADC and sent to the computer for FT [4] in order to yield the conventional spectrum [28].

1.4 High Magnetic Fields

The presence of a magnetic field is vital for studying the characteristics of materials in many scientific disciplines because many physical phenomena depend explicitly on it. Achieving high magnetic fields [40] is possible by using superconducting magnets, which were developed during the 1960s using superconducting wires [5]. A superconducting magnet is an electromagnet made from coils of superconducting wire (superconductor) which must be cooled to cryogenic temperatures using LHe during operation. In the superconducting state, the wire has no electrical resistance and therefore, can conduct much larger electric currents than ordinary wire, creating intense magnetic fields. An important characteristic of any superconductor is the maximum electric transport current density that the superconductor is able to maintain without resistance [41].

Unlike permanent magnets, superconducting magnets allow easy tuning and inverting of the magnetic field. However, the use of cryogenic fluids, such as LN_2 (77 K) and LHe (4.2 K), is inevitable for their operation, which is in case of LHe quite expensive. Operating and maintaining these magnets in laboratories requires a dedicated infrastructure (helium recovery system, liquefiers) and periodic transfer of cryogenc fluids by trained personnel [42]. Nonetheless, with the development of cryogen-free superconducting magnets in recent years [42] – [44], experiments in high magnetic fields have become feasible also for facilities without LHe infrastructure. Cryogen-free superconducting magnets are becoming popular due to their relatively simple and less costly operation compared to conventional LHe-cooled ones [42].

2 FTIR Magneto-Spectroscopy

This chapter focuses on the key method of this doctoral thesis, Fourier Transform Infrared Spectroscopy (FTIR) in high magnetic fields, also referred to as FTIR magneto-spectroscopy, which deals with the study of materials in magnetic fields using FTIR spectroscopy.

Spectroscopy is one of the most fundamental and widespread experimental techniques for scientific investigation. Spectroscopy performed in the IR range is particularly informative due to numerous intrinsic material responses associated with intra-band electronic transitions, collective modes, and the interaction of radiation with lattice vibrations, i.e., phonons [45]. The presence of a magnetic field is essential for studying the characteristics of materials because many physical phenomena depend explicitly on it. In general, magneto-optical experiments provide powerful tools for gaining insights into the properties of materials, and such experiments are often an ideal way to study new physical phenomena. For instance, the IR region in magnetic fields is particularly important since it covers the magnetic resonances and other important effects [5, 6] illustrated in Fig. 2.1.

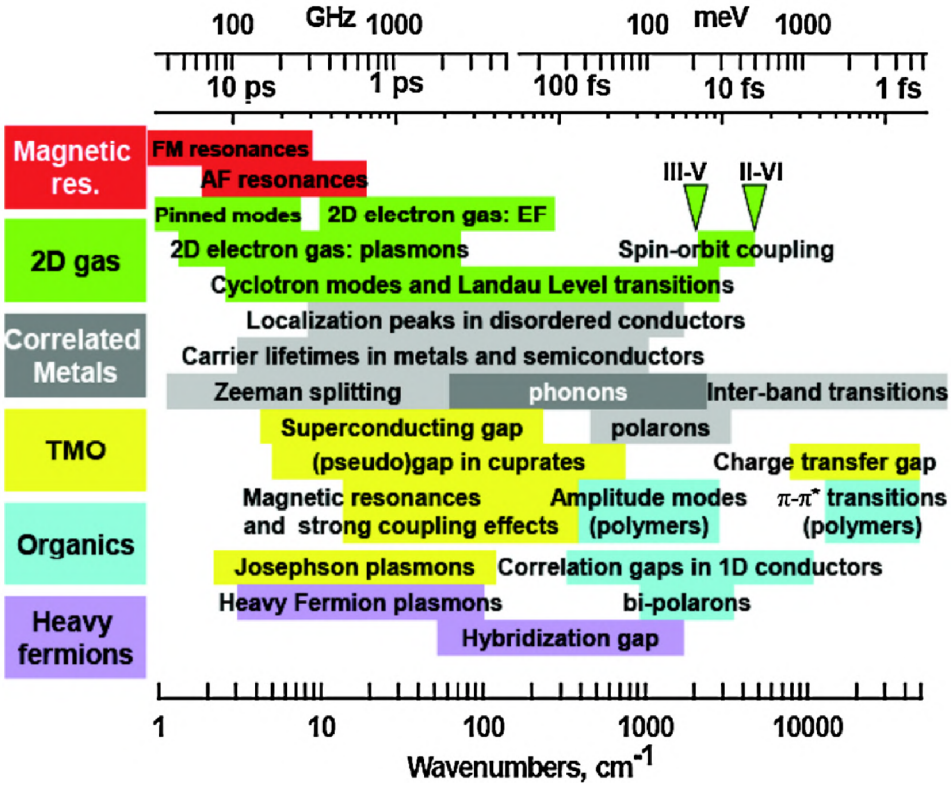

Fig. 2.1: Schematic representation of magnetic field-induced phenomena observable in the IR range. Taken from [6].

Historically, the first magneto-optical measurements in the IR range were performed in the 1950s to elucidate phenomena such as cyclotron resonance [46,47], antiferromagnetic (AF) resonance [48], later in the 1960s, electron paramagnetic resonance (EPR) [49], then in the 1970s, transitions between Landau Levels (LLs) [50,51], Bardeen–Cooper–Schrieffer (BCS) superconductivity, 2D electron gas/plasmon–phonon interaction, etc. [45]. The importance of magneto-optical measurements has not diminished over the years. FTIR magneto-spectroscopy is still a powerful spectroscopic technique (especially at low temperatures) for investigating many important physical phenomena (see Fig. 2.1) and elucidating the exotic behavior of novel materials, which are currently of great interest, such as single-molecule magnets (SMMs) [10] – [21], graphene [22] – [27], topological insulators [52,53], Weyl semimetals [54,55], or superconductors [56].

Our research is aimed mainly at the investigation of spin-related EPR transitions/energy splittings in transition metal compounds and other paramagnetic materials such as SMMs, molecules displaying slow relaxation of magnetization of purely molecular origin [7], thus the ability to store one bit of information at much higher densities, using FTIR magneto-spectroscopy.

In addition to SMMs, our research also focuses on investigating the band structure and electronic properties of 2D materials such as graphene [22] – [27] using FTIR magneto-spectroscopy, which probes dipole magneto-optical transitions of electrons, such as transitions between LLs.

The following sections explain the physical principles of the phenomena underpinning our research, i.e., EPR and transitions between LLs. We also describe in detail the most relevant class of materials for our research, i.e., SMMs.

2.1 Electron Paramagnetic Resonance (EPR)

Electron Paramagnetic Resonance (EPR), sometimes called Electron Spin Resonance (ESR), spectroscopy is a powerful technique for studying magnetic and electronic properties of materials with unpaired electrons, i.e., paramagnetic materials, such as paramagnetic complexes, radicals or defects in crystals [57]. EPR is resonant absorption of usually microwave radiation by paramagnetic molecules or ions with at least one unpaired electron spin in the presence of a static magnetic field [57]. It is based on the Zeeman effect that is the separation of the energy of spin states in the presence of a magnetic field. In the simplest case of a free electron, where B designates the magnetic field that satisfies the resonance condition, can be expressed as

$$\Delta U = h\nu = g_e \mu_B B, \tag{2.1}$$

where h is Planck constant, $g_e = 2.0023$ is the free-electron g-factor and μ_B is Bohr magneton. For free unpaired electrons, it means that the splitting of the energy levels is directly proportional to the magnetic field, as shown in Fig. 2.2. Transitions between the two electronic Zeeman levels are then induced by electromagnetic radiation of the appropriate frequency ν such that the photon energy $h\nu$ matches the energy-level separation ΔU [57].

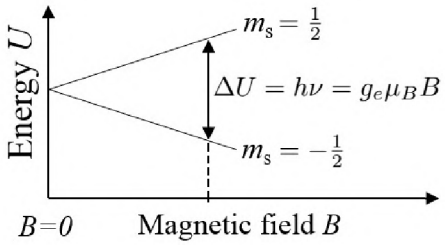

Fig. 2.2: Zeeman splitting of electron spin states. Energy diagram for a free electron in magnetic field B.

EPR spectroscopy is a fundamental spectroscopic technique for determining the physical chemical properties of paramagnetic coordination compounds and molecular magnetic materials. These compounds frequently exhibit EPR transitions over a wide range of energies, corresponding to frequencies from MHz to THz. SMMs are a special class of materials belonging to the paramagnetic coordination compounds that particularly benefit from EPR as they usually possess large zero-field splitting (ZFS). Primary sources of these energy splittings are spin-orbit and spin-spin interactions among unpaired electrons that can lead to ZFS of ground-state magnetic sublevels [58, 59]. However, conventional microwave EPR systems do not provide experimental access to the EPR transitions of SMMs with large ZFS, which are currently of interest. FTIR magneto-spectroscopy enables us to observe EPR transitions of SMMs with large ZFS, mainly based on transition metal complexes [10] – [17] or lanthanides [18] – [21], in which conventional microwave EPR systems do not provide experimental access to the magnetic resonance transitions. Moreover, it is an essential method in the characterization of SMMs due to the ability to probe molecular and electronic properties directly [8, 9].

2.1.1 Single-Molecule Magnets (SMMs)

Due to their nanometer dimensions and the ability to store one bit of information using individual spins[1], molecular species built up of paramagnetic transition metals or lanthanide metal ions called SMMs give a possibility to move technology forward. Their molecular nature offers unique attributes that allow them to store information with much higher density. The first example of SMMs was Mn(III) cluster [Mn_{12}OAc], see Figure 2.3 (a), in which slow relaxation of the magnetization was observed and published in *Nature* in 1993 [60]. Since then, they have drawn the increasing attention of the scientific community [61] – [65] due to their potential applications in high-density data storage [66], quantum computing [67], and spintronics [68, 69].

The key feature of SMMs is the slow relaxation of the magnetization of purely molecular origin [7]. Commonly used characteristic quantities, which basically describes the quality of SMMs, are the blocking[2] temperature T_B and the effective energy barrier U_{eff} [19]. The energy barrier corresponds to the separation between the positive and negative magnetization states of a SMM. Consequently, at low temperatures, the system is trapped in one of the high-spin energy wells, see Figure 2.3 (b). The higher the barrier, the longer a material remains magnetized, therefore U_{eff} should be as large as possible [73].

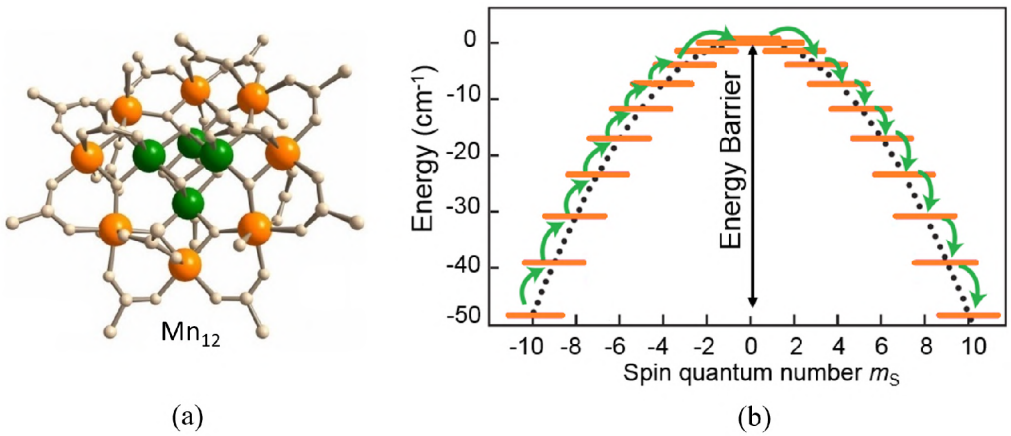

Fig. 2.3: (a) The first SMMs – molecule Mn_{12} in which slow relaxation of the magnetization at low temperature was observed in 1993. Taken from [71]. (b) Potential energy as a function of the spin quantum number. Adapted from [72].

[1] by assigning binary 0 to one orientation of the magnetic moment, and binary 1 to its opposite orientation

[2] maximum temperature at which it is possible to observe hysteresis in the field-dependence of the magnetization [70].

Traditionally, the energy barrier U_{eff} of first row transition metals SMMs is estimated as $U_{eff} = S^2|D|$ and $U_{eff} = (S^2 - 1/4)|D|$ for integer and non-integer spin respectively [7]. In these equations, S is the total spin of the complex (spin of the ground state), and D is the magnetic anisotropy constant called the axial term of the second rank ZFS tensor [10]. ZFS is a phenomenon arising in paramagnetic systems with multiple unpaired electrons (S > 1/2) as a result of spin-orbit coupling (SOC) and spin-spin coupling (SSC) interactions, and interaction with ligands. SOC is the interaction of the (unpaired) electron spin angular momentum with the electron orbital angular momentum, and SSC is the direct, dipolar interaction among pairs of unpaired electrons [74], and/or exchange interactions. Magnetic anisotropy is the preferential alignment of the magnetic moment along a specific direction so-called easy axis[3] or alternatively easy plane [7]. To improve the energy barrier, scientists from the beginning focused on increasing the total spin. However, recently it was realized that with increasing S, D actually decreases, and the energy barrier does not improve much [75,76]. Therefore, attention turned to systems with large magnetic anisotropies D [10], especially lanthanides (f-block elements). Since 2003, when the slow relaxation of the magnetization was observed in lanthanide-based SMM by Ishikawa [77], lanthanide-based complexes are intensively investigated, and they have already yielded promising results. Slow relaxation of magnetization at the temperature above liquid nitrogen (80 K) was observed in lanthanide-based SMMs in 2018 [70]. This observation denoted a huge success in the field of molecular magnetism, since the main drawback of SMMs, which stands in the way of moving these molecules out of the lab to applications, is that they exhibit magnetic memory effects usually only in cryogenic temperatures.

An essential class of SMMs are mononuclear[4] complexes called Single-Ion Magnets (SIMs), that exhibit slow magnetic relaxation in the absence of the magnetic field. The single ion in SIMs can be transition metal ion, but also lanthanide-based ion. SIMs represent the most straightforward model systems based on which the physics of spin, anisotropy, and magnetic relaxation in metal complexes can be probed and understood. Hence, the study of SIMs properties and their behavior can be considered as a fundamental undertaking in the quest to fabricate functional nanoscale magnetic materials from the bottom-up [7].

Mononuclear transition-metal complexes are of current interest in molecular magnetism due to their intriguing physical properties, such as magnetic bistability[5] at low temperatures, or quantum tunneling of magnetization, and promising applications [16]. There has been a growing number of first-row/3 d-block SIM systems

[3] The most energetically favourable direction of spontaneous magnetization in a system [7].
[4] They contain only a single paramagnetic ion.
[5] They exhibit an energy barrier to spin reversal from $+M_s$ to $-M_s$ [7].

reported in the literature last years. Cobalt complexes attract significant attention due to their frequently very large magnetic anisotropies [78].

In general, transition metal complexes can be separated into half-integer spin states (S= 1/2, 3/2, etc.) and integer-spin states (S = 1, 2, etc.) [79]. According to the Kramers theorem, spin levels of half-integer spin state (Kramers) ions are in the absence of an external magnetic field at least doubly degenerate. An external magnetic field removes the remaining degeneracy of the Kramers doublets. In contrast, integer spin state (non-Kramers) ions are split by ZFS to nondegenerate spin levels [80], see Fig. 2.4.

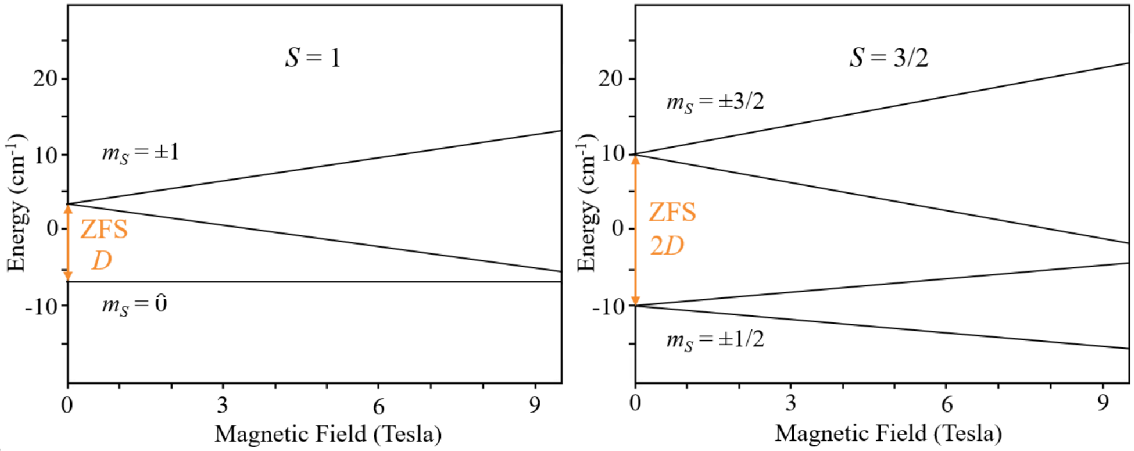

Fig. 2.4: Simulated spin sublevel energies as a function of a magnetic field with indicated ZFS (D and $2D$, respectively) for the two simplest HS ions : S = 1 (left, representing the non-Kramers class), and S = 3/2 (right, representing the Kramers class). An axial ZFS tensor was assumed in both cases, with $D = 10\,\mathrm{cm}^{-1}$ and $E = 0\,\mathrm{cm}^{-1}$, together with isotropic g = 2.00, $B_0 \parallel z$.

From the point of view of EPR spectroscopy (not coordination chemistry), transition metal complexes can also be divided into two classes: low-spin (LS), with S = 1/2 (as S = 0 is diamagnetic and useless for EPR), and high-spin (HS), with S > 1/2. The main difference between LS and HS complexes is that the phenomenon of ZFS only appears in HS states [79]. Since the presence of the ZFS phenomenon is essential for the determination of SMMs properties, only HS systems are relevant in this regard.

The magnetic behavior of SIMs with HS state (the interaction with nuclear spins are neglected) is governed by spin Hamiltonian in the form:

$$\hat{H} = \hat{H}_{Zee} + \hat{H}_{ZFS} = \mu_B \hat{\boldsymbol{S}} \boldsymbol{g} \boldsymbol{B_0} + \hat{\boldsymbol{S}} \boldsymbol{D} \hat{\boldsymbol{S}}, \tag{2.2}$$

where $\hat{H}_{Zee}$ denotes the electron-Zeeman interaction, and $\hat{H}_{ZFS}$ the ZFS, with $\boldsymbol{D}$ being ZFS tensor [80]. It is convenient to define $\boldsymbol{D}$ in a local frame, where $\boldsymbol{D}$ is diagonal with D_x, D_y, D_z are the principal values of ZFS tensor, and z-axis is the main anisotropy axis, then the ZFS spin Hamiltonian can be expressed as:

$$\hat{H}_{ZFS} = D[\hat{S}_z^2 - \frac{1}{3}S(S+1)] + E(\hat{S}_x^2 - \hat{S}_y^2), \tag{2.3}$$

where $\hat{S}$ is a spin operator, which describes the spin projection along a given axis, and $D = 3/2D_z$ and $E = (D_x - D_y)/2$ are the axial and rhombic ZFS parameters, respectively [80]. The role of D and E is to lift the degeneracy of the $2S + 1$ spin microstates/sublevels associated with a given S even in the absence of an external magnetic field. For more detailed insight into the ZFS phenomenon and relationship between D and E, see ref. [74].

Accurate determination of the spin Hamiltonian parameters in transition metal complexes with large ZFS might be challenging in studying magnetic and spectroscopic properties of HS transition metal complexes [16]. Complexes with HS states frequently exhibit EPR transitions over a wide range of energies, corresponding to frequencies from a few hundred MHz to a few THz. For precise determination of spin transition energies by EPR, frequency of the applied radiation has to match the transition energy of interest. This can be problematic to accomplish in the case of systems with very large ZFS, or systems with unknown spin transition energies. One possibility to meet this challenge is to use high-field/high-frequency EPR (HFEPR) spectroscopy, which uses a single fixed frequency[6] in combination with a very broad field scans (0 – 25 T). An alternative approach is to use FTIR magneto-spectroscopy, which employs scans of the exceptionally broad frequency range (up to hundreds cm^{-1}, far beyond the range of routine EPR spectrometers) at a set of fixed magnetic fields, so the possibility to match the desired frequency is much higher. This approach can be beneficial for so-called "EPR silent" systems (usually integer-spin states), which show no EPR transitions in conventional X-band (9 – 10 GHz/ 0 – 1 T) and Q-band (33 – 35 GHz/0 – 2 T) spectrometers. Additionally, an important advantage of FTIR magneto-spectroscopy in high magnetic fields is that the ZFS can often be extracted directly from the zero-field spectrum [59].

To sum up, a substantial contribution of FTIR magneto-spectroscopy is studying EPR transitions in paramagnetic compounds, particularly multinuclear HS systems (SMMs) and mononuclear complexes (SIMs) based on transition metal ions [10] – [17], and lanthanides [18] – [21] distributed over a broad transition-energy range, which is challenging or even impossible with other, more conventional EPR techniques [8, 9].

[6] typically in the 100 – 1000 GHz range

2.2 Landau Levels (LLs)

The cyclotron resonance phenomenon originates from the quantization of the cyclotron orbits and energy levels of electrons subjected to intense magnetic fields, also known as Landau quantization.

If we consider a charged particle, e.g. an electron with the elementary charge e and instantaneous velocity v in an electric field E and a uniform magnetic field B, the Lorentz force F_L[7], on it is given by:

$$F = e[E + (v \times B)]. \tag{2.4}$$

The magnetic force that is always perpendicular to the velocity of a charged particle, acting on the free electron with mass m, will a cause circular motion. The frequency of this circular motion is called cyclotron frequency ω_c. It is given by equation

$$\omega_c = \frac{eB}{m}. \tag{2.5}$$

In many semiconductors, it is possible to determine the effective masses of carriers in the conduction and valence bands near the band edges by cyclotron resonance. For these materials, mass of charged particle m in equation 2.6 is then replaced by the appropriate cyclotron effective mass m^* [81].

Under high magnetic fields, such orbits become quantized, and associated quantized energy levels are called Landau levels (LLs). The quantized energies are given by [39]:

$$E_n = (n + 1/2)\hbar\omega_c, \text{ where } n = 0, 1, 2, ... \tag{2.6}$$

Cyclotron resonance is then the resonant absorption of light/energy with a frequency equal to the frequency difference between LLs. The LLs are degenerate, with the number of electrons per level directly proportional to the strength of the applied magnetic field. Landau quantization is directly responsible for oscillations in the electronic properties of materials as a function of the applied magnetic field, such as Shubnikov-de Haas or De Haas-van Alpen phenomenon [82, 83].

[7] the combination of electric and magnetic force on a point charge due to electromagnetic fields

3 Experimental Setup

As explained in the previous chapter, FTIR magneto-spectroscopy is a powerful spectroscopic technique used to investigate many important effects in materials, e.g., electron spin resonance, cyclotron resonance, and transitions between Landau levels (LLs). Despite their enormous potential in material science, infrared magneto-spectrometers are still relatively rare and custom-made since such systems generally require complex infrastructure. In this chapter, we describe the design and implementation of a versatile broadband setup for for FTIR magneto-spectroscopy, FTIR magneto-spectroscopic setup, spanning the range from THz/FIR to NIR, 50 –10,000 cm^{-1} (200 – 1 μm, 6.2 – 1,240 meV, 1.5 – 300 THz), high magnetic field up to 16 T, and cryogenic temperatures down to 2 K. Our FTIR magneto-spectroscopic setup, shown in Fig. 3.1, is based on a commercially available FTIR spectrometer Bruker Vertex 80v (Bruker Corporation, Billerica, USA) and a 16 T cryogen-free

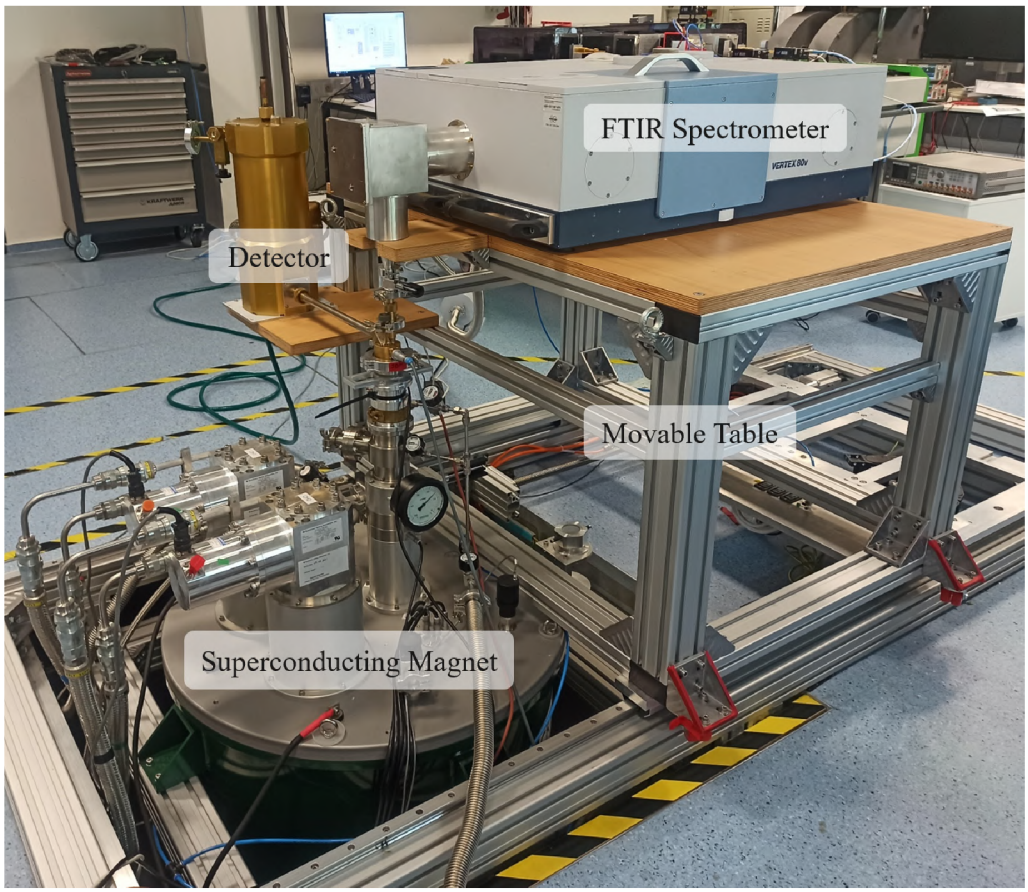

Fig. 3.1: Photograph of the FTIR magneto-spectroscopic setup at the Central European Institute of Technology of the Brno University of Technology (CEITEC BUT). The setup is in the configuration with Probe A and 1.6 K standard bolometer system.

superconducting magnet (Cryogenic Ltd., London, UK). We constructed custom-designed optics that couple the spectrometer to the superconducting magnet. It consists of optical coupling and transmission probes (A and B) designed for magneto-optical measurements with multiple detectors. Using various detectors, the setup spans the entire IR and partially the THz range. This aspect is particularly important because it enables the measurement of different types of samples from SMMs in the FIR region to germanium in the NIR region, as demonstrated in the chapter of magneto-optical measurements. Another novelty of the setup lies in the usage of a cryogen-free superconducting magnet. Additionally, the setup includes a home-built movable table on which the FTIR spectrometer, the optical coupling, and the detectors are placed.

3.1 Beam Propagation

The schematic of the FTIR magneto-spectroscopic setup in Fig. 3.2 shows the beam propagation through the setup in two configurations of detector placement. The beam originates in the spectrometer's source and passes through the aperture (APT = 8 mm) and beamsplitter (BMS) of the Michelson interferometer. Then, the parallel beam is guided out through an output of the spectrometer (OUT 2) to the optical coupling, in which the parallel beam from the spectrometer is reflected from the parabolic mirror at 90° and focused to its focal point located in a gate valve. When the gate valve is closed, the spectrometer and the optical coupling are evacuated to about 2 mbar pressure. The rough vacuum reaches the probe's window when the transmission probe is connected, and the gate valve is opened. After inserting the transmission probe through an airlock into a variable temperature insert (VTI) of the superconducting magnet, helium gas fills the probe. The windows in the setup, made of 35 μm thick mylar foil, keep the helium gas inside the probe and separate it from the optical coupling and surrounding environment. Two transmission probes can be attached to the optical coupling:

a) **Probe A:** In this configuration, the detector (D) is placed outside the magnet, see Fig. 3.2(a). The beam enters the first tube and passes through the window (W). Then, it is transmitted through a sample (S) located approximately in the center of the magnetic field. At the bottom of the probe, the transmitted beam is reflected by two 90° flat mirrors (M) and propagates up through a second tube. At the end of the second tube, another 90° flat mirror (M) is located, which reflects it to a third, horizontal, tube. At the end of this tube, the beam passes through another window and goes to the detector (D).

b) **Probe B:** In this configuration, the detector (D) is placed inside the supercon-

ducting magnet, see Fig. 3.2(b). The beam enters the tube by passing through the window (W) and propagates to a sample (S) located in the center of the magnetic field. The transmitted beam from the sample (S) goes to the detector (D) placed below the sample.

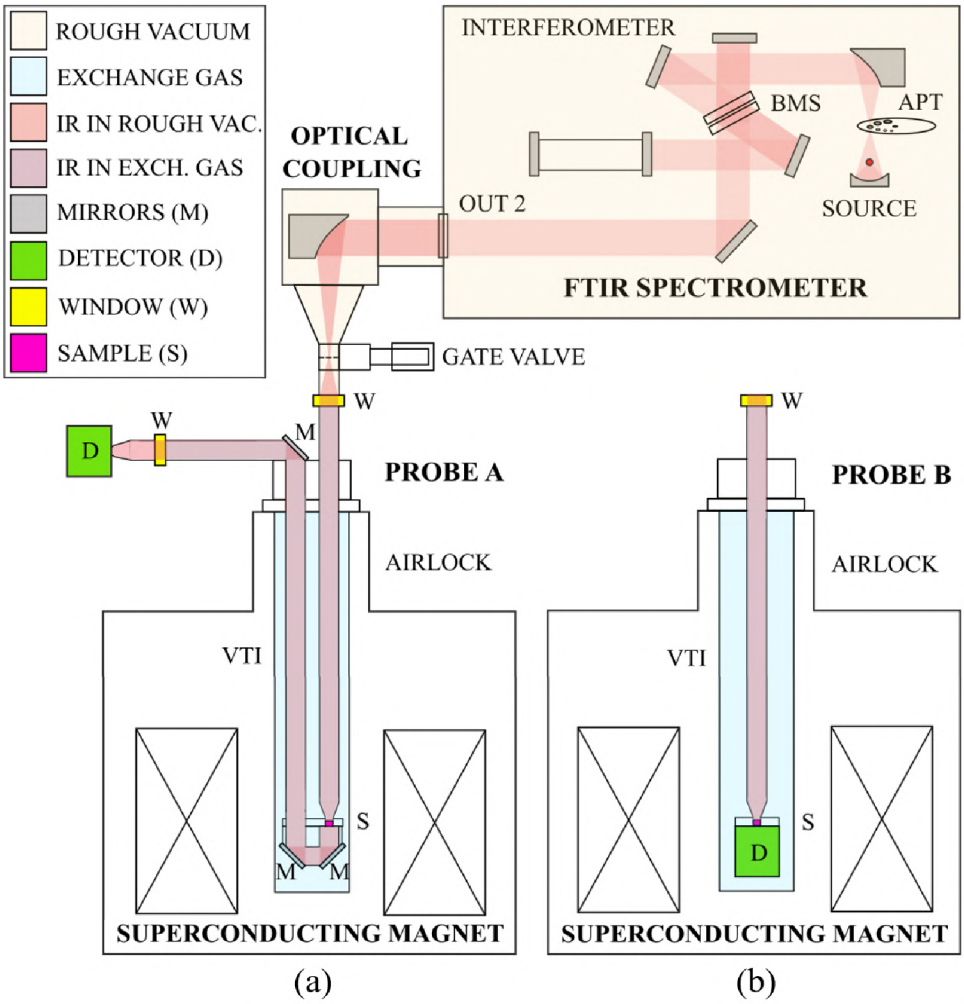

Fig. 3.2: The schematic of the FTIR magneto-spectroscopic setup shows the beam propagation through the setup in two configurations of the detector location. (a) Probe A, inserted into the superconducting magnet, is designed for the detector located outside the magnet, and (b) Probe B is designed for the detector located inside the magnet. (VTI in the figure stands for variable temperature insert, BMS stands for beamsplitter, and APT stands for aperture.)

3.2 Setup Design and Components

When designing the custom-designed parts of the setup, the emphasis was to ensure that all components were made from non-magnetic materials, i.e., brass, bronze,

aluminum, and non-magnetic stainless steel (316L), to avoid possible complications from strong forces caused by stray fields of the magnet. Another criterion for material choice was the suitability for cryogenic temperatures. The setup's components are sealed with o-rings ensuring rough vacuum conditions.

3.2.1 FTIR Spectrometer

Our experimental setup utilizes a FTIR spectrometer Bruker Vertex 80v designed for spectroscopic measurements under vacuum conditions. The settings and measurements are controlled by spectroscopic software OPUS 7. The spectrometer is currently equipped with:

- **Sources**: standard MIR (Globar), and NIR source (tungsten halogen lamp).
- **Beamsplitters (BMS):** CaF_2 for NIR (1,200 – 15,000 cm^{-1}), standard KBr for MIR (350 – 8,000 cm^{-1}), Mylar Multilayer for FIR range (30 – 680 cm^{-1}).
- **Detectors:** There are standard detectors operating at room temperaturesupplied together with the spectrometer: NIR InGaAs (4,000 – 12,800 cm^{-1}), MIR-DTGS (250 – 12,000 cm^{-1}), FIR-DTGS (10 – 700 cm^{-1}).
  There is a possibility to use detectors operating at low temperatures, which were purchased additionally and can be connected to the spectrometer: a pumped LHe-cooled 1.6 K standard bolometer system (Infrared Laboratories, Tuscon, USA) for the FIR range (5 – 670 cm^{-1}), and a 4.2 K sealed general purpose bolometer with 3 mm diamond absorber (Infrared Laboratories, Tuscon, USA) for FIR, MIR and NIR ranges (10 – 2,000 cm^{-1})[1], which is designed to operate inside the superconducting magnet.

3.2.2 Superconductive Magnet

Our setup utilizes 16 T cryogen-free superconducting solenoid magnet from Cryogenic Ltd. equipped with two pulse cryocoolers and integrated variable temperature insert (VTI) with ⌀50 mm sample space, which enables control of the temperature inside the magnet between T = 1.8–320 K. The VTI incorporates a home-built airlock port for probe insertion, avoiding contamination of the closed-cycle helium environment by pumping and flushing the probe space before sliding into the operation position through the opened VTI valve [84].

3.2.3 Optical Coupling

The optical coupling (see Fig. 3.3) is designed to reflect the parallel beam from

[1] This range of the bolometer was provided by the manufacturer, but the bolometer worked far above this range.

the spectrometer using a parabolic mirror and focus it to the transmission probe inserted into the superconducting magnet. Its main purpose is to enable proper alignment of the parabolic mirror to ensure effective coupling of the probes. The optical coupling consists of a guiding tube that is connected to the output (OUT 2) of the spectrometer , a parabolic mirror housing, a focusing cone mounted on the bottom of the housing, and a gate valve VATLOCK (VAT group AG, Haag, Switzerland) with inner diameter ⌀15.1 mm with a manual actuator. Inside the parabolic mirror housing, a precision kinematic mirror mount (Thorlabs, Newton, NJ, USA) is mounted. The mirror mount holds ⌀76.2 mm 90° off-axis gold-coated parabolic mirror with RFL = 228.6 mm (Thorlabs, Newton, NJ, USA).

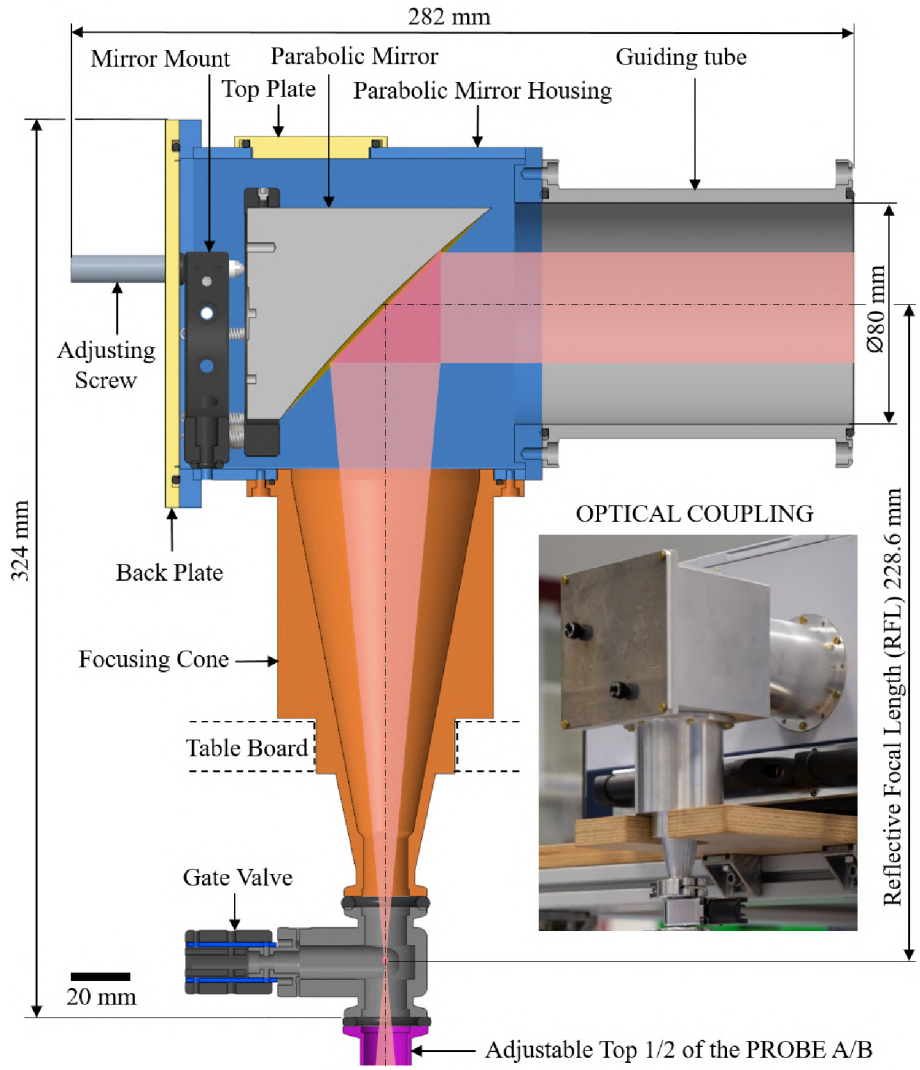

Fig. 3.3: The scheme of the optical coupling design. The optical coupling reflects the parallel beam from the spectrometer using a parabolic mirror and focuses it to Probe A or B inserted into the superconducting magnet.

3.2.4 Transmission Probes

Transmission probes incorporate waveguides, in other words, or light pipes, which are tubes guiding the beam through a sample (reference) placed in the magnetic field to the detector. To reach stable cryogenic temperatures at a sample, it is necessary to reduce the heat flow from the top of the probe, which is at room temperature, to the probe tubes and a sample located inside the cryogenic helium environment. Therefore, the tubes in our setup are made of non-magnetic stainless steel (316L) due to its relatively low thermal conductivity compared with other materials traditionally used for waveguides, e.g., Nickel silver. These tubes were additionally polished inside to improve the reflectivity (to improve reflectivity even more, it is possible to coat the tubes internally with a gold layer in the future). The tubes of inner diameter 15 mm were chosen to fit two tubes side by side into the VTI with the maximal possible diameter based on the assumption that there are fewer reflections in the larger diameter tubes and thus fewer losses. Probe A - External Detection Probe is shown in Fig. 3.4, Probe B - Internal Detection Probe is shown in Fig. 3.5, and Probe B - Chipset Probe (see Fig. 3.6) is created from Probe B by attaching the chip sample holder [85, 86] with graphene bolometer devices [87–89] instead of the sealed bolometer and replacing a few other parts.

3.3 Performance of the Setup

We have characterized the performance of the FTIR magneto-spectroscopic setup in several different configurations depending on the probe, source, beamsplitter, and detector choice. The results from these tests are summarized in Tab. 3.1, in which typical operating spectral ranges for beamsplitters, detectors, operating temperature ranges for detectors, and possible sample temperatures are depicted. We demonstrate the performance of the setup by the power spectrum, which depicts intensity versus wavenumber and the so-called 100% line, which is a typical indicator of the noise level of the spectroscopic system [4]. 100% line is obtained by measuring a transmission spectrum (spectrum 1) and then dividing it by a subsequent spectrum (spectrum 2). In the ideal case, the division should be a straight line at 100%. The deviation from this line represents the noise and instability of the system as a function of wavenumber (frequency) [45]. 100% line clearly displays the performance and workable setup range (fifth column of the table) for each configuration. To compare the performance between configurations in the specific IR range, 100% line spectra are plotted with the same y-axis range, ±1% for the NIR configurations, ±10% for the MIR and FIR configurations. These measurements were performed on an empty opening (reference) at zero magnetic field. All spectra were acquired with

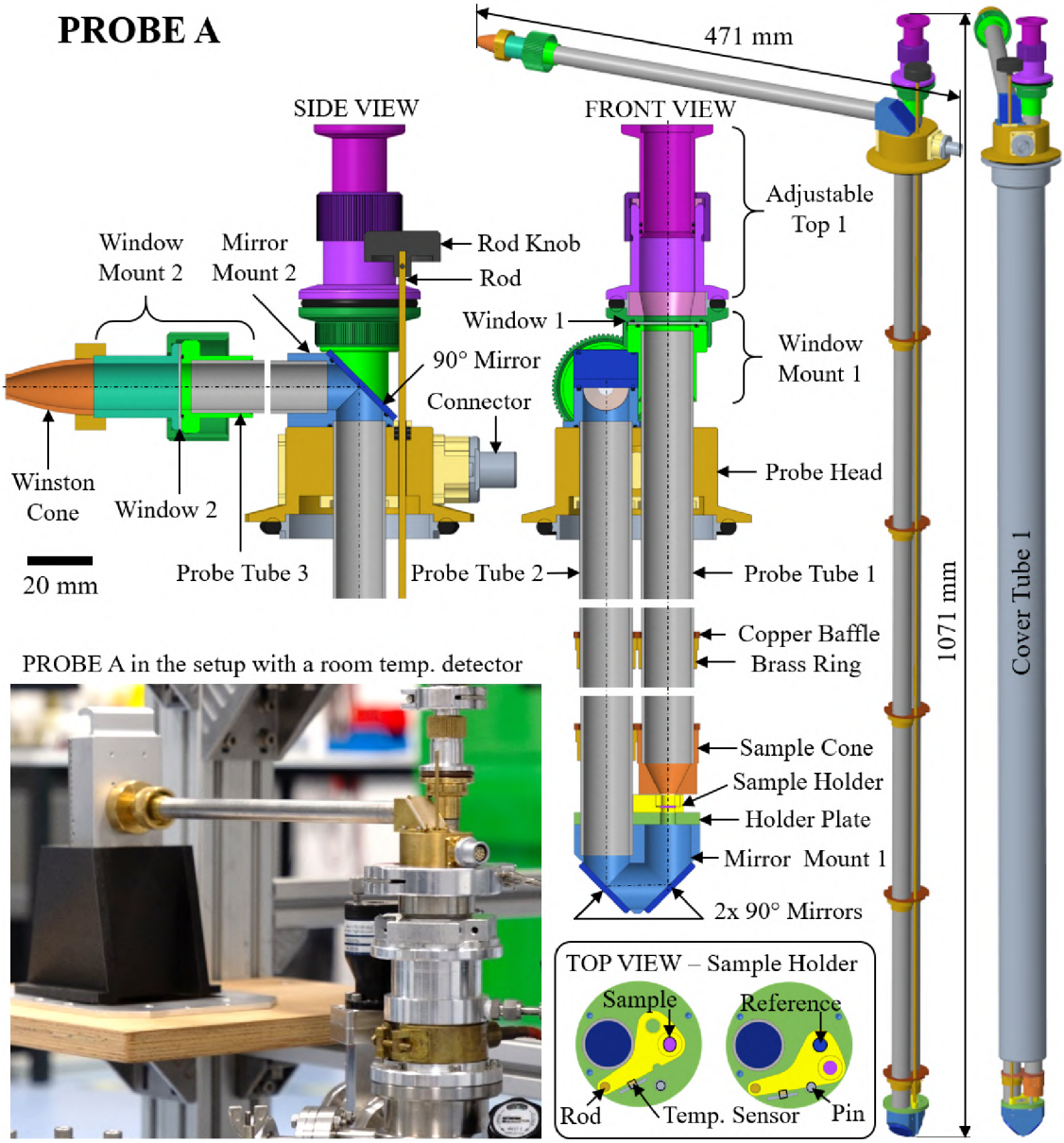

Fig. 3.4: The scheme of Probe A - External Detection Probe design with its cross-section, side views, and top view on the sample holder. This transmission probe is used as waveguides guiding the beam through a sample/reference in the magnetic field to the detector placed outside the magnet. The photograph inset displays the top parts of Probe A.

the same scanning time (10 min) and resolution (1 cm^{-1}). The interferometer scan speed f_{SCN} displayed in the power spectra was optimized for each detector based on its characteristics. As expected, the performance of the setup in configurations with room temperature FIR-DTGS and MIR-DTGS detectors is clearly worse than with using LHe-cooled detectors in the FIR and MIR ranges. In all presented confi-

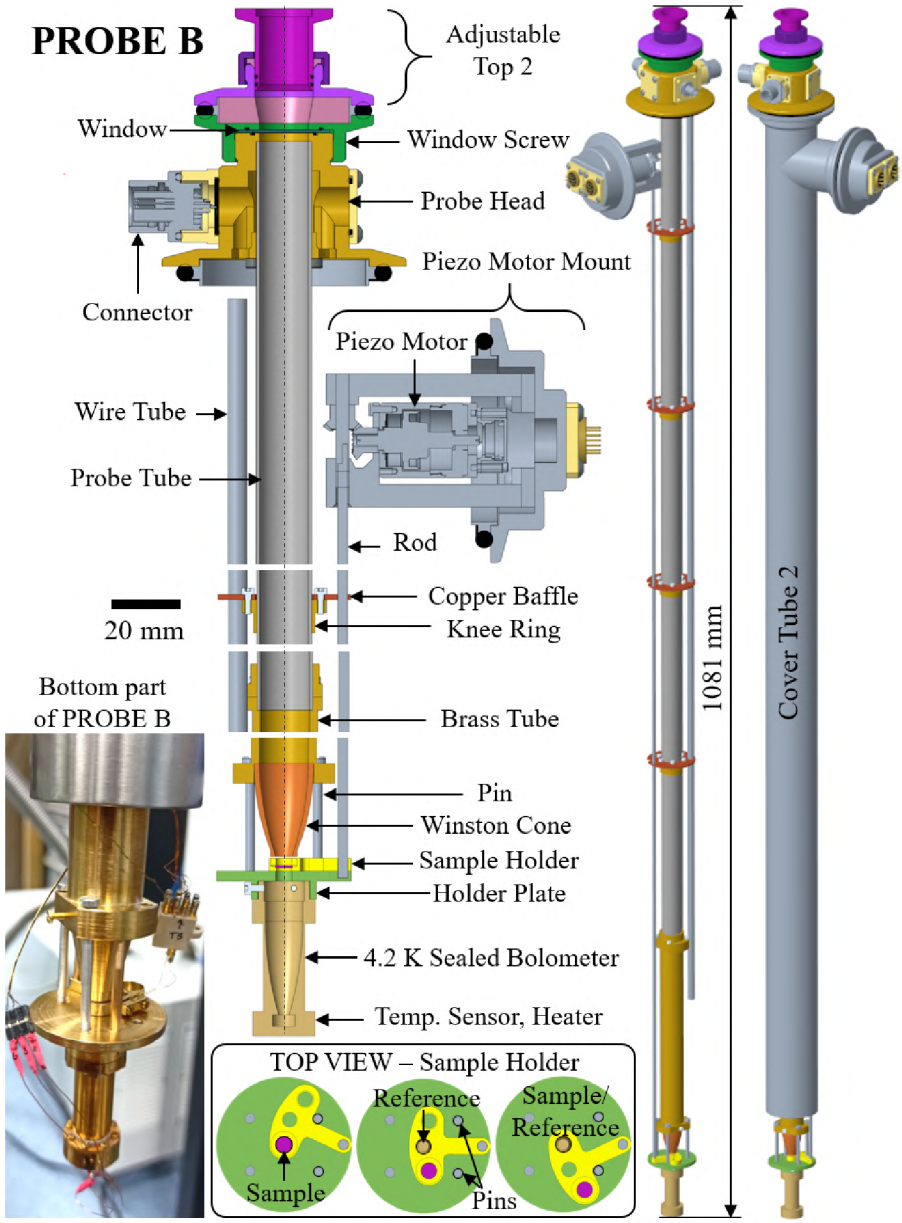

Fig. 3.5: The scheme of Probe B - Internal Detection Probe design with its cross-section, side views, and top view on the sample holder. This transmission probe is used as waveguides guiding the beam through a sample/reference in the magnetic field to the detector placed inside the superconducting magnet. The photograph inset displays the bottom parts of Probe B.

gurations, mylar foil (35 μm) windows were used in the setup, but they can be easily replaced with windows made of other materials. We have chosen mylar due to its wide frequency range where it can be used. However, mylar caused typical absorptions around 1,500 cm^{-1} and 3,000 cm^{-1} visible in the MIR range power spectra and noise peaks in 100% line.

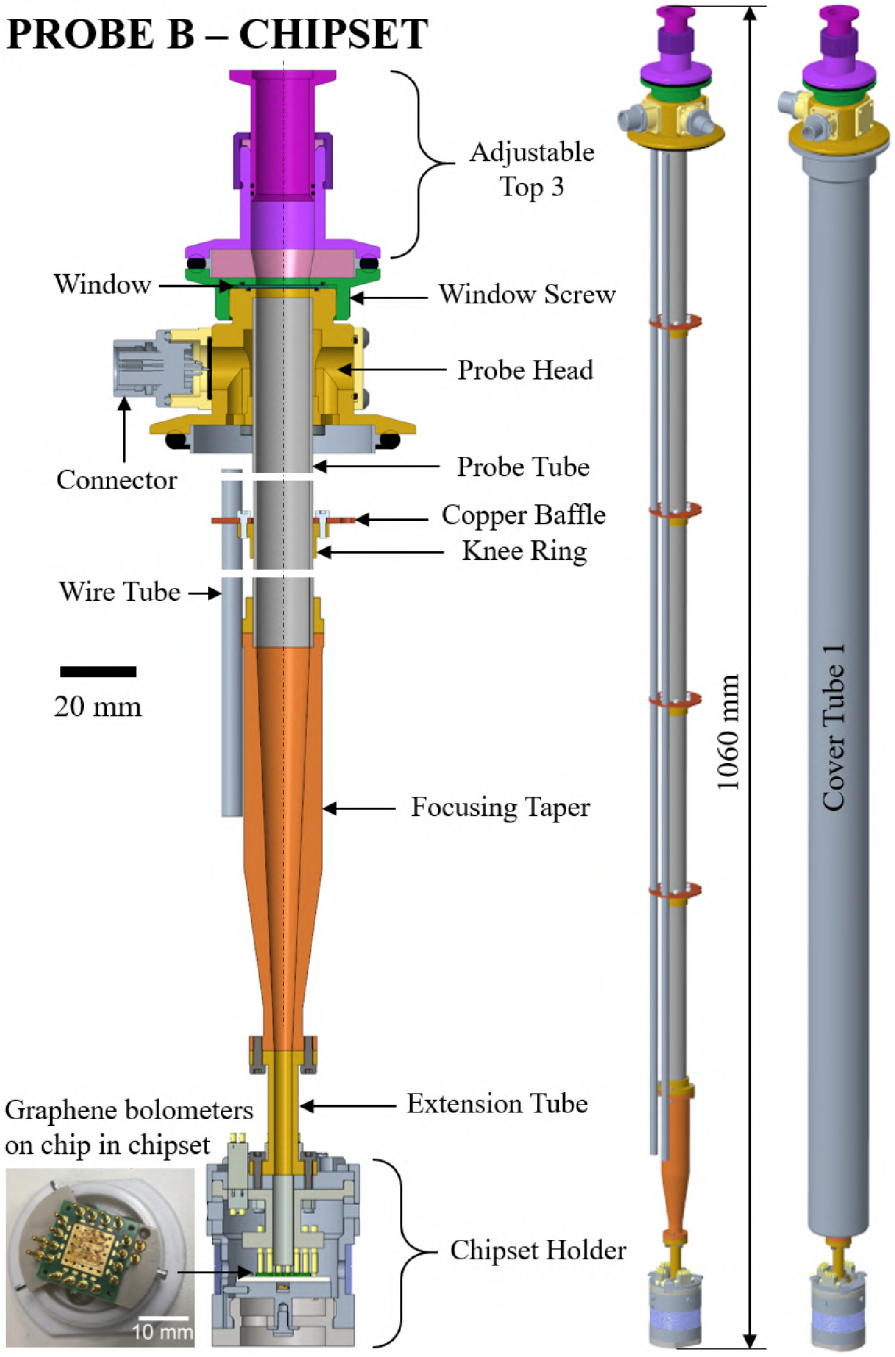

Fig. 3.6: The scheme of Probe B - Chipset Probe design with its cross-section and side views. This probe is used as a waveguide guiding the beam onto the graphene bolometric devices on the chip of the chipset holder placed inside the superconducting magnet. The photograph inset displays the graphene bolometers on the chip in the chipset.

Probe	Source	Beamsplitter Range (cm^{-1})	Detector Range (cm^{-1}) (Oper. temp.)	Setup range (cm^{-1})	Sample temp. (K)	Power Spectrum	100% Line
A	Tungsten	CaF_2 1,200 – 15,000	InGaAs 4,000 – 12,800 (Room Temp.)	**NIR** 4,000 – 10,000	2 – 320	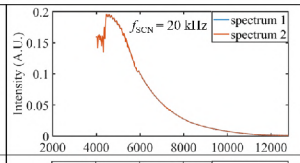	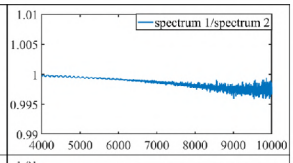
B	Tungsten	CaF_2 1,200 – 15,000	4.2 K Scaled Bolometer 10 – 2,000* (LHe-cooled)	**NIR** 2,000 – 8,000	4.2	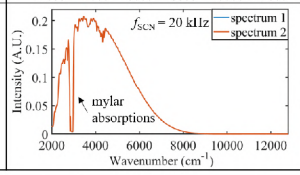	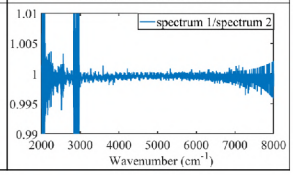
A	Globar	KBr 350 – 8,000	MIR-DTGS 250 – 12,000 (Room Temp.)	**MIR** 400 – 5,000	2 – 320	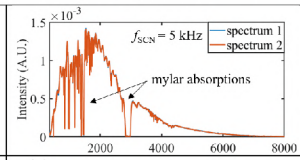	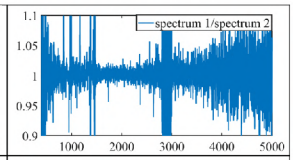
B	Globar	KBr 350 – 8,000	4.2 K Sealed Bolometer 10 – 2,000* (LHe-cooled)	**MIR** 400 – 4,000	4.2	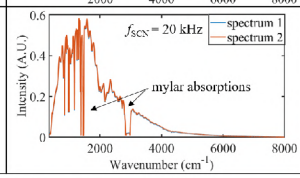	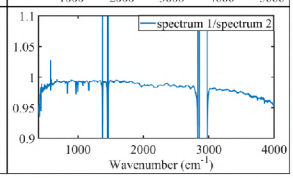
A	Globar	Mylar Multilayer 30 – 680	FIR-DTGS 10 – 700 (Room Temp.)	**FIR** 150 – 680	2 – 320	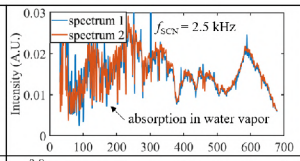	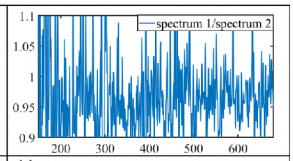
A	Globar	Mylar Multilayer 30 – 680	1.6 K Standard Bolometer 5 – 670 (LHe-cooled)	**FIR** 50 – 670	2 – 320	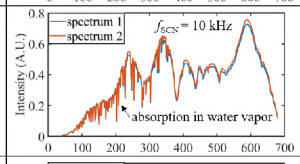	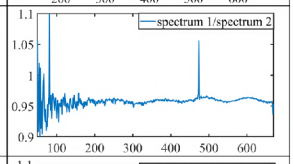
B	Globar	Mylar Multilayer 30 – 680	4.2 K Scaled Bolometer 10 – 2,000* (LHe-cooled)	**FIR** 50 – 680	4.2	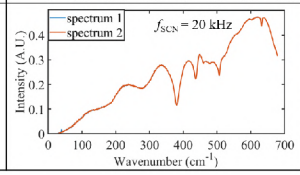	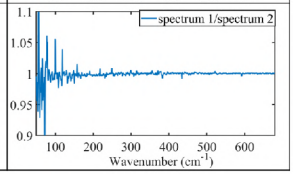

Tab. 3.1: All possible configurations of the FTIR magneto-spectroscopic setup according to the choice of the probe, source, beamsplitter, and detector, with spectral and sample temperature ranges, and corresponding power spectrum (intensity vs. wavenumber) together with 100% line, obtained as the division of spectrum 1 by a subsequent spectrum 2. (*This range of the bolometer was provided by the manufacturer, but the bolometer worked far above this range.)

4 Magneto-Optical Measurements

Following magneto-optical measurements on the FTIR magneto-spectroscopic setup located at CEITEC BUT. We demonstrate the functionality of the FTIR magneto-spectroscopic setup in various configurations on several different samples, i.e. SIM, germanium. The magneto-optical response of the studied samples has been explored in the THz/IR range, using the standard Faraday configuration. In the FIR range, we used globar source and LHe-cooled bolometers for SIM sample, and room temperature DTGS detector for graphene. In the NIR range, we used Tungsten lamp and room temperature InGaAs detector to measure germanium. Data from magneto-optical measurements presented in this section were obtained using Labview program (created by Ing. Matúš Šedivý) that combines control of the superconducting magnet and the FTIR spectrometer.

4.1 Zero-field Splitting in Cobalt(II)-based SIM

Following results were obtained in cooperation and published in *IEEE Transactions on Instrumentation and Measurement (TIM)* [14]:
Dubnická Midlíková, J.; Šedivý, M.; Sojka, A.; Tadeu Santana, V.; Dubroka, A.; Neugebauer, P. A Versatile Setup for FTIR Magneto-Spectroscopy *IEEE Transactions on Instrumentation and Measurement*. 2023, vol. 72, pp. 1-11. https://doi.org/10.1109/TIM.2023.3284943.

Abstract

Fourier-transform infrared (FTIR) magneto-spectroscopy is a powerful spectroscopic technique used to investigate many important effects in materials, e.g., electron spin resonance, cyclotron resonance, and transitions between Landau levels. Despite their enormous potential in material science, infrared magneto-spectrometers are still relatively rare and custom-made since such systems generally require complex infrastructure. This article presents a broadband setup for FTIR magneto-spectroscopy spanning the range from THz/far-infrared (FIR) to near-infrared (NIR), high magnetic field up to 16 T, and cryogenic temperatures down to 2 K. It consists of a commercial FTIR spectrometer and 16 T cryogen-free superconducting magnet coupled with custom-designed optical coupling and transmission probes for experiments with various detectors. The versatility of the FTIR magneto-spectroscopic setup is demonstrated by the magneto-optical measurements on a cobalt-based single-molecule magnet in the FIR and germanium in the NIR range.

The functionality of the FTIR magneto-spectroscopic setup was demonstrated on two samples. The first sample was a representative of SIM with very large ZFS, which was measured in the FIR range on the magneto-optical setup at GHMFL; results of these measurements can be found in [12] for complex labeled as **3**. We chose this sample (identical 12 mg pellet) so we can compare the results obtained from our setup in the FIR range with those previously published. By the magneto-optical measurements of complex **3**, we tested the setup in the FIR region.
For cobalt(II) complexes with $S = 3/2$, the ZFS between two Kramers doublets is equal to $2(D^2 + 3E^2)^{1/2}$. This energy gap is then directly observable in FTIR magneto-optical spectra as $2D$ (when omitting rhombicity E).

The spectra of pressed powder pellet of pentacoordinate cobalt(II)-based complex **3** ([$Co(L2)Cl_2$], where L2 = 2,6-bis(1-dodecyl-1H-benzimidazole-2-yl)-pyridine, were recorded in Probe A configuration with 1.6 K standard bolometer in the FIR range at T = 2 K, and magnetic fields B up to 16 T. The spectra were measured with resolution 4 cm^{-1}, same as in [12] and resolution 1 cm^{-1}. Since the peaks are very narrow, resolution 1 cm^{-1} was found to be more suitable than resolution 4 cm^{-1}. The transmission spectra of the sample at magnetic field (T_B) were normalized by the zero-field transmission spectra of the sample (T_0), T_B/T_0. Normalized relative transmission spectra, see Fig. 4.1, are depicted in the form of a color map in Fig. 4.2 for better identification of the EPR transitions. Color maps of the normalized relative transmission spectra show a clear field-dependence of one of the peaks starting at ~186 cm^{-1} at zero magnetic field attributed to the EPR transition from $m_s = \pm 3/2$ to $m_s = \pm 1/2$ states. In Fig. 4.2, we applied the same simulation as in [12] calculated using the EasySpin Toolbox for Matlab [59] based on the SH and the parameters $E/D = 0.162$, $D = -89$ cm^{-1}, $g_{iso} = 2.1$. In addition, we normalized the data as T_B/T_{B+1} and applied the same simulation to confirm the peak position. Red color of the simulation represents the strongly allowed transitions; grey color indicates forbidden/weakly allowed transitions. The spectra obtained on our setup at CEITEC BUT shown in Fig. 4.2 are almost identical to those obtained at GHMFL. In all color maps, the tendency toward the yellow color means the absorption is suppressed by the magnetic field, whereas the dark blue color means the absorption is induced by the magnetic field.

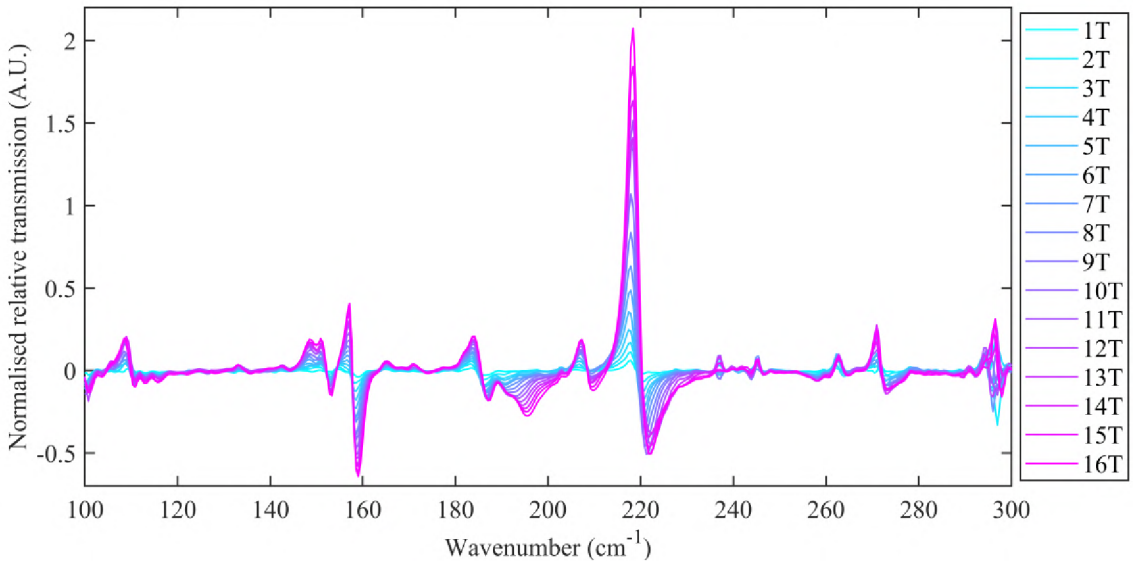

Fig. 4.1: Normalized relative transmission spectra (with baseline correction) recorded on pressed powder pellet of complex **3** at T = 2 K and magnetic field up to 16 T and resolution 1 cm^{-1} on the FTIR magneto-spectroscopic setup at CEITEC BUT. The spectra at magnetic field (T_B) were normalized by the zero-field transmission spectra (T_0), T_B/T_0.

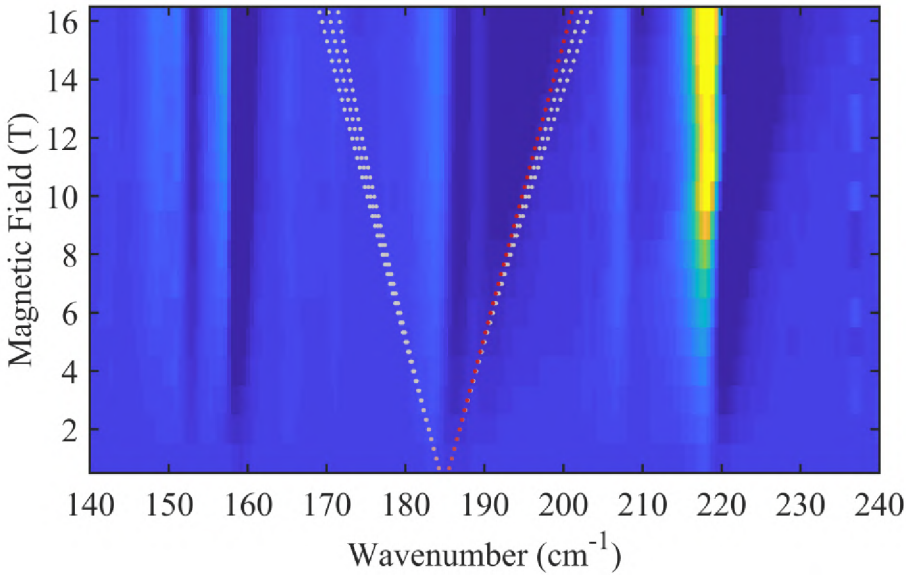

Fig. 4.2: A color map of normalized relative transmission spectra recorded on pressed powder pellet of **3** measured at T = 2 K, magnetic field up to 16 T, and resolution 1 cm^{-1} obtained on our FTIR magneto-spectroscopic setup.

4.2 Indirect Interband Transitions between LLs in Germanium

Following results were obtained in cooperation and published in *IEEE TIM* [14]: **Dubnická Midlíková, J.**; Šedivý, M.; Sojka, A.; Tadeu Santana, V.; Dubroka, A.; Neugebauer, P. A Versatile Setup for FTIR Magneto-Spectroscopy *IEEE Transactions on Instrumentation and Measurement*. 2023, vol. 72, pp. 1-11. https://doi.org/10.1109/TIM.2023.3284943.

Since these results were published in the same publication as the results from the previous subsection entitled Zero-field Splitting in Cobalt(II)-based SIM, the abstract is given in section 4.1.

The functionality of the FTIR magneto-spectroscopic setup was demonstrated on two samples. The second sample was a well-known indirect band gap semiconductor – germanium (Ge), measured in the NIR range to observe the magneto-optical response of its absorption edge. We chose Ge due to its well-studied band structure and the amount of available literature [90], [91].
Using the FTIR magneto-spectroscopy, we can probe the band structure, e.g., Landau levels (LLs), and elucidate the electronic properties of 2D materials such as graphene [22] – [27], or semiconductors such as germanium [90], [91], [92].

The magneto-optical spectra were acquired on a very weakly p-type galium-doped Ge ($\rho = 11\,\Omega$cm, p = 2x10^{14} cm^3) (100) wafer at 5 K in the magnetic field B up to 16 T with Probe A and InGaAs room temperature detector in the NIR region. Fig. 4.3 shows normalized relative transmission spectra (T_B/T_0) of Ge measured with resolution 8 cm^{-1} at 64 values of applied magnetic fields B from 0.25 T to 16 T with step 0.25 T plotted with an offset for clarity. The spectra are shown in the range of absorption edge of Ge at low temperatures. The maxima correspond to individual inter-LL transitions. The minima correspond to the suppression of zero-field absorption. Normalized relative transmission spectra from Fig. 4.3 were visualized as a color map shown in Fig. 4.4(a). Fig. 4.4(b) displays a color map of the second derivative of these normalized relative transmission spectra to enhance fine structures, e.g. the splitting of LL transitions. The maxima of the signal in Fig. 4.4(b) are shown in Fig. 4.4(c).

They were analyzed using the model of transitions between LLs of parabolic bands [93]:

$$E_N = \Delta E_N + (N + \frac{1}{2})\hbar\omega_c, \tag{4.1}$$

where $N = 0, 1, 2, \ldots$ is the index of a LL, ΔE_N is the energy value at $B = 0$, $\omega_c = eB/\mu$ is the cyclotron frequency, e is the elementary charge, and μ is the re-

duced effective mass. Parabolicity of the bands leads to the linear dependence of the energy of absorption lines to the magnetic field, which is well fulfilled in the whole measured range. The model employs three different reduced effective masses, $\mu_1 = (0.128 \pm 0.015)\, m$, $\mu_2 = (0.132 \pm 0.016)\, m$, $\mu_3 = (0.138 \pm 0.014)\, m$ where m is the free electron mass, to account for the small splitting of LL, which becomes apparent for $N > 3$. The Landau level with $N = 0$ has a different value of $\Delta E_{N=0} = 769\,\mathrm{meV}$ than for $N > 3$, $\Delta E_{N>0} = 773\,\mathrm{meV}$. The latter indicates that a different phonon mediates $N = 0$ transition than $N > 0$ transitions. Considering the value of the band gap of Ge at low temperatures of 741 meV [94], the energy of phonons amounts to 28 meV for $N = 0$ transition and 32 meV for $N > 0$ transitions. The three values of reduced effective masses compare well with the electron effective masses obtained by Dresselhaus *et al.* for the sample with a magnetic field tilted by a few degrees from the (001) direction, see Fig. 5 in Ref. [90]. Surprisingly, the obtained effective masses compare well with the electron effective mass rather than with the reduced effective mass $1/\mu = 1/m_{hh} + 1/m_e$, which is expected for an indirect transition between the heavy hole band with effective hole mass $m_{hh} = 0.29\, m$ and the conduction band with effective electron mass $m_e = 0.13\, m$ for B in 001 direction. We tentatively interpret this observation as a transition between localized hole states (with a very large effective mass) to the conduction band.

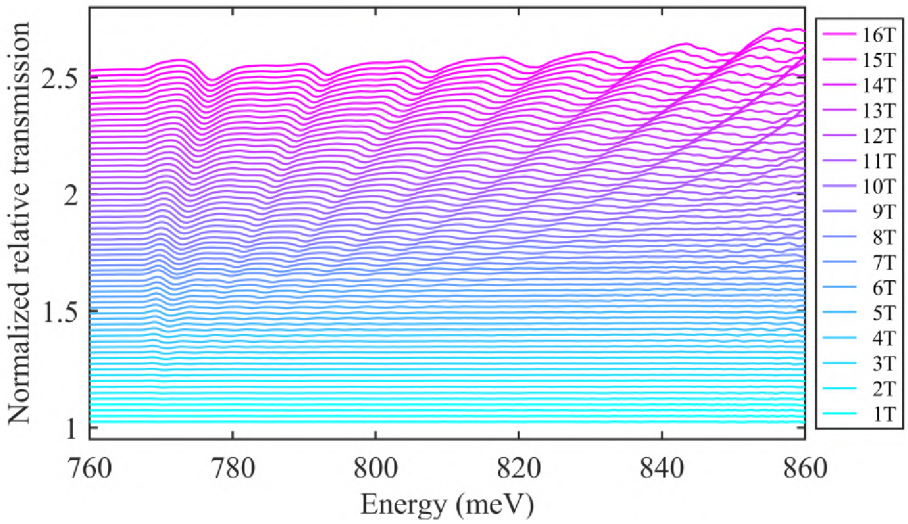

Fig. 4.3: Normalized relative transmission spectra, T_B/T_0, plotted with an offset for 64 values of applied magnetic fields from 0.25 T to 16 T with step 0.25 T. The maxima correspond to individual inter-LL transitions, and the minima emerge due to the suppression of the zero-field absorption.

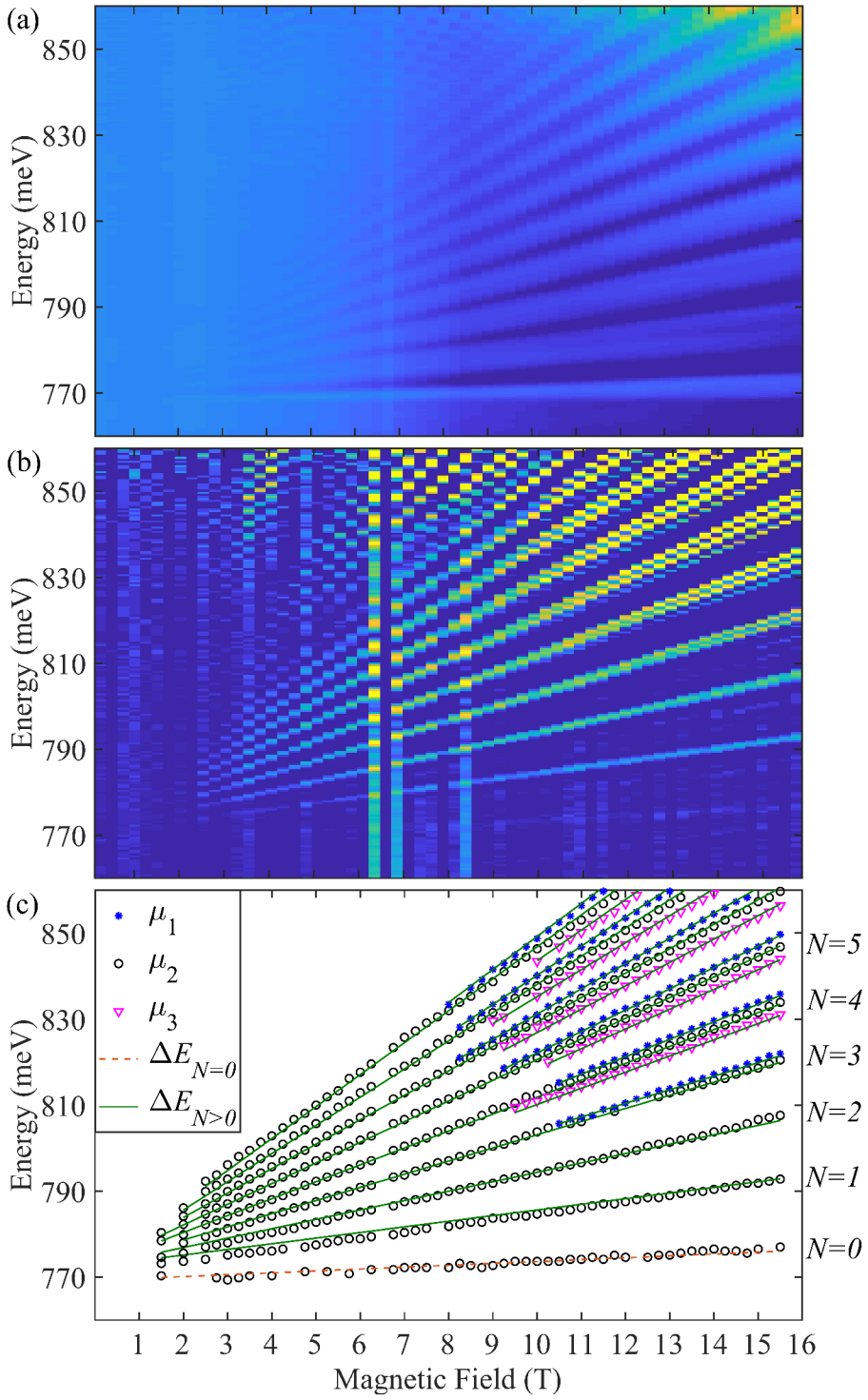

Fig. 4.4: (a) A color map of normalized relative transmission spectra from Fig. 4.3, (b) a color map of the second derivative of normalized relative transmission spectra from (a). (c) The minima of (b) fitted with a model of LL transitions as described in the text. Three markers correspond to three values of reduced effective mass. The solid and dashed lines correspond to two values of ΔE_N.

Conclusion and Outlook

In this doctoral thesis, we have explored the use of FTIR magneto-spectroscopy as a powerful method for studying the properties of various materials, including SMMs and 2D materials. In order to fulfill the main goal of the thesis, we have developed the versatile FTIR magneto-spectroscopic setup to mediate this method at CEITEC BUT and perform sensitive magneto-optical measurements.

In the first two chapters, we provided the theoretical background with key concepts that underpin our research topic. We firstly introduced electromagnetic radiation, IR spectroscopy, FTIR spectrometer and high magnetic fields. The second chapter was dedicated to the FTIR magneto-spectroscopy method itself and its applications.

In the third chapter, we have described in detail the design and implementation of the home-build versatile FTIR magneto-spectroscopic setup, which is based on a commercial FTIR spectrometer and the cryogen-free superconducting magnet coupled with the optical coupling and transmission probes for experiments with various detectors thanks to which the setup spans the entire IR and partially the THz range. This aspect is particularly important because it enables the measurement of different types of samples, demonstrated in the fourth chapter. A novelty of the setup lies in the usage of a cryogen-free superconducting magnet, which is a very convenient choice for facilities without LHe infrastructure. Within this chapter, we have tested the performance of the FTIR magneto-spectroscopic setup at zero magnetic field for various configurations to determine a usable setup range.

Last but not least, the fourth chapter of the thesis provided experimental results of magneto-optical measurements at CEITEC BUT performed on our FTIR magneto-spectroscopic setup. These results include the magneto-optical measurements by which the functionality of our setup was demonstrated, i.e., the ZFS in cobalt(II)-based single ion magnet in the FIR region, and indirect inter-band transitions between Landau levels (LLs) in germanium in the NIR region.

To sum up, in this doctoral thesis we presented FTIR spectroscopy in high magnetic fields/FTIR magneto-spectroscopy as a powerful spectroscopic technique used to investigate many important effects in materials, e.g., EPR in SMMs with very large ZFS, mainly based on transition metal complexes or lanthanides, in which conventional microwave EPR systems do not provide experimental access to the magnetic resonance transitions, and transitions between LLs of semiconductors or 2D materials such as graphene. Furthermore, we have described in detail the versatile FTIR magneto-spectroscopic setup operating in the range 50–10,000 cm^{-1}, temperatures between 2–320 K, and magnetic fields up to 16 T located at CEITEC

BUT. We have designed versatile FTIR magneto-spectroscopic setup using several methods, and have tested its performance of the at zero magnetic field for various configurations to determine a workable setup range summarized in Tab. 3.1. The functionality of the setup has been demonstrated on magneto-optical measurements of cobalt(II)-based SIM in the FIR region, and germanium in the NIR region. The measurements of SIM have shown that the setup provides high-quality spectra and results comparable to those performed on a similar setup at GHMFL. In germanium, we observed indirect inter-band transitions between LLs and analyzed them with a model yielding three values of reduced effective masses.

In the context of prospective advancements, the flexibility of the FTIR magneto-spectroscopic setup enables further development and improvements, such as the implementation of new sample holders for different types of measurements, internal coating of waveguides with a layer of gold or silver to further enhance the transmission, etc. Our group focuses on the studies of SMMs and high-spin coordination compounds with large ZFS, including transition metals and lanthanides, exploring the physics behind their behavior still rarely reported at those energy ranges. Furthermore, the presented versatile setup allows performing field-induced measurements on 2D devices [87,88], e.g., by shifting the Fermi level in semiconductors, and electrically detected magnetic resonance (EDMR), which may lead to interesting discoveries. Moreover, we are interested in exploring the properties in topological materials or Weyl semimetals, which are known to exhibit exotic electronic properties under applied magnetic fields [52, 54].

Thanks to its relatively simple design and implementation of a cryogen-free superconducting magnet, the presented FTIR magneto-spectroscopic setup paves the way for other research institutions without the LHe infrastructure to perform IR magneto-optical experiments in high magnetic fields.

References

[1] CHRISTY, A. A., OZAKI, Y. and GREGORIOU, V. G. *Modern fourier transform infrared spectroscopy*. New York: Elsevier, 2001. ISBN 978-0444500441.

[2] HERSCHEL, W. Experiments on the refrangibility of the invisible rays of the sun. (1800). *Philosophical Transactions of the Royal Society of London*. 1800, vol. 90, pp. 284–292. DOI: 10.1098/rstl.1800.0015.

[3] DERRICK, M. R., STULIK, D. and LANDRY, J. M. *Infrared spectroscopy in conservation science*. Los Angeles: Getty Conservation Institute, 1999. ISBN 0-89236-469-6.

[4] GRIFFITHS, P. R. and DE HASETH, J. A. *Fourier transform infrared spectrometry*. 2nd ed. Hoboken, N.J.: Wiley-Interscience, 2007. ISBN 978-0-471-19404-0.

[5] *High magnetic field science and its application in the United States: current status and future directions*. Washington, D.C.: The National Academies Press, 2013. ISBN 978-0-309-28634-3.

[6] BASOV, D. N., AVERITT, R. D., VAN DER MAREL, D., DRESSEL, M., and HAULE, K. Electrodynamics of correlated electron materials. *Reviews of Modern Physics* 2011, vol. 83, no. 2, pp. 471–541. DOI: 10.1103/RevModPhys.83.471.

[7] FROST, J. M., HARRIMAN, K. L. M. and MURUGESU, M. The rise of 3-d single-ion magnets in molecular magnetism: towards materials from molecules?. *Chemical Science*. 2016, vol. 7, no. 4, pp. 2470-2491. DOI: 10.1039/C5SC03224E.

[8] NEHRKORN, J., HOLLDACK, K., Robert BITTL, R., SCHNEGG, A. Recent progress in synchrotron-based frequency-domain Fourier-transform THz-EPR. *Journal of Magnetic Resonance*. 2017, vol. 280, pp. 10-19. DOI: 10.1016/j.jmr.2017.04.001.

[9] WINPENNY, R. and AROMÍ, G. *Single-molecule magnets and related phenomena*. New York: Springer, 2006. ISBN 3540332391.

[10] RECHKEMMER, Y., BREITGOFF, F. D., VAN DER MEER, M., ATANASOV, M., HAKL, M., ORLITA, M., NEUGEBAUER, P., NEESE, F., SARKAR, B., VAN SLAGEREN, J. A four-coordinate cobalt(II) single-ion magnet

with coercivity and a very high energy barrier, *Nature Communications*. 2016, vol. 7, no. 10467. DOI: 10.1038/ncomms10467.

[11] BAMBERGER, H., ALBOLD, U., DUBNICKÁ MIDLÍKOVÁ, J., SU, C.-Y., DEIBEL, N., HUNGER, D., HALLMEN, P. P., NEUGEBAUER, P., BEERHUES, J., DEMESHKO, S., MEYER, F., SARKAR, B., VAN SLAGEREN, J. Iron(II), Cobalt(II), and Nickel(II) Complexes of Bis(sulfonamido)benzenes: Redox Properties, Large Zero-Field Splittings, and Single-Ion Magnets, *Inorganic Chemistry*. 2021, vol. 60, no. 5, pp. 2953–2963. DOI: 10.1021/acs.inorgchem.0c02949.

[12] JURÁKOVÁ, J.; DUBNICKÁ MIDLÍKOVÁ, J.; HRUBÝ, J.; KLIUIKOV, A.; SANTANA, V. T.; PAVLIK, J.; MONCOL, J.; ČIŽMÁR, E.; ORLITA, M.; MOHELSKÝ, I.; NEUGEBAUER, P.; GENTILI, D.; CAVALLINI, M.; ŠALITROŠ, I. Pentacoordinate cobalt(II) single ion magnets with pendant alkyl chains: shall we go for chloride or bromide? *Inorganic Chemistry Frontiers*. 2022, vol. 9, pp. 1179–1194, DOI: 10.1039/D1QI01350E.

[13] MALINOVÁ, N., JURÁKOVÁ, J., BRACHŇAKOVÁ, B., DUBNICKÁ MIDLÍKOVÁ, J., ČIŽMÁR, E., SANTANA, V. T., HERCHEL, R., ORLITA, M., MOHELSKÝ, I., MONCOL, J., NEUGEBAUER, P., ŠALITROŠ, I. Magnetization Slow Dynamics in Mononuclear Co(II) Field-Induced Single-Molecule Magnet, *Crystal Growth & Design*. 2023, vol. 23, iss. 4, pp. 2430–2441. DOI: 10.1021/acs.cgd.2c01388.

[14] DUBNICKÁ MIDLÍKOVÁ, J., ŠEDIVÝ, M., SOJKA, A., TADEU SANTANA, V., DUBROKA, A., NEUGEBAUER, P. A Versatile Setup for FTIR Magneto-Spectroscopy *IEEE Transactions on Instrumentation and Measurement*. 2023, vol. 72, pp. 1-11. DOI: 10.1109/TIM.2023.3284943.

[15] LIU, J.-J., MENG, Y.-S., HLAVIČKA, I., ORLITA, M., JIANG, S.-D., WANG, B.-W., GAO, S. "Determination of zero-field splitting in Co^{2+} halide complexes with magnetic and far-IR measurements. *Dalton Transactions*. 2017, vol. 46, no.23, pp. 7408-7411. DOI: 10.1039/C7DT01486D.

[16] MISOCHKO, E. Y., AKIMOV, A. V., KORCHAGIN, D. V., NEHRKORN, J., OZEROV, M., PALII, A. V., CLEMENTE-JUAN, J. M., ALDOSHIN, S. M. Purely Spectroscopic Determination of the Spin Hamiltonian Parameters in High-Spin Six-Coordinated Cobalt(II) Complexes with Large Zero-Field Splitting. *Inorganic Chemistry*. 2019, vol. 58, no. 24, pp. 16434-16444. DOI: 10.1021/acs.inorgchem.9b02195.

[17] MOSELEY, D. H., STAVRETIS, S. E., THIRUNAVUKKUARASU, K., OZEROV, M., CHENG, Y., DAEMEN, L. L., LUDWIG, J., LU, Z., SMIRNOV, D., BROWN, C. M., PANDEY, A., RAMIREZ-CUESTA, A. J., LAMB, A. C., ATANASOV, M., BILL, E., NEESE, F., XUE, Z.-L. Spin–phonon couplings in transition metal complexes with slow magnetic relaxation, *Nature Communications*. 2018, vol. 9, no. 2572. DOI: 10.1038/s41467-018-04896-0.

[18] MARX, R., MORO, F., DÖRFEL, M., UNGUR, L., WATERS, M., JIANG, S. D., ORLITA, M., TAYLOR, J., FREY, W., CHIBOTARU, L. F., VAN SLAGEREN, J. Spectroscopic determination of crystal field splittings in lanthanide double deckers. *Chemical Science*. 2014, vol. 5, no. 8. DOI: 10.1039/c4sc00751d.

[19] HAAS, S. *Far-infrared spectroscopy of lanthanide-based molecular magnetic materials*. 2015. Dissertation. University of Stuttgart. Available from: https://elib.uni-stuttgart.de/handle/11682/5178.

[20] LIDDLE, S. T. and VAN SLAGEREN, J. Improving f-element single molecule magnets. *Chemical Society Reviews*. 2015, vol. 44, no. 19, pp. 6655-6669. DOI: 10.1039/C5CS00222B.

[21] KRAGSKOW, J. G. C., MARBEY, J., BUCH, C. D., NEHRKORN, J., OZEROV, M., PILIGKOS, S., HILL, S., CHILTON, N. F. Analysis of vibronic coupling in a 4f molecular magnet with FIRMS. *Nature Communications*. 2022, vol. 13, no. 825. DOI: 10.1038/s41467-022-28352-2.

[22] NEUGEBAUER, P., ORLITA, M., FAUGERAS, C., BARRA, A.-L., POTEMSKI, M. How Perfect Can Graphene Be? *Physical Review Letters*. 2009, vol. 103, no. 13. DOI: 10.1103/PhysRevLett.103.136403.

[23] SADOWSKI, M. L., MARTINEZ, G., POTEMSKI, M., BERGER, C., DE HEER, W. A. Landau Level Spectroscopy of Ultrathin Graphite Layers. *Physical Review Letters*. 2006, vol. 97, no. 26. DOI: 10.1103/physrevlett.97.266405.

[24] JIANG, Z., HENRIKSEN, E. A., TUNG, L. C., WANG, Y.-J., SCHWARTZ, M. E., HAN, M. Y., KIM, P., STORMER, H. L. Infrared spectroscopy of Landau levels in graphene. *Physical Review Letters*. 2007, vol. 98, no. 19. DOI: 10.1103/PhysRevLett.98.197403.

[25] NEDOLIUK, I. O., HU, S., GEIM, A. K., KUZMENKO, A. B. Colossal infrared and terahertz magneto-optical activity in a two-dimensional Dirac material. *Nature Nanotechnology*. 2019, vol. 14, pp. 756–761. DOI: 10.1038/s41565-019-0489-8.

[26] CRASSEE, I., LEVALLOIS, J., WALTER, A. L., OSTLER, M., BOSTWICK, A., ROTENBERG, E., SEYLLER, T., VAN DER MAREL, D., KUZMENKO, A. B. Giant Faraday rotation in single- and multilayer graphene. *Nature Physics*. 2011, vol. 7, pp. 48-51. DOI: 10.1038/nphys1816.

[27] ORLITA, M., FAUGERAS, C., PLOCHOCKA, P., NEUGEBAUER, P., MARTINEZ, G., MAUDE, D. K., BARRA, A.-L., SPRINKLE, M., BERGER, C., DE HEER, W. A., POTEMSKI, M. Approaching the Dirac Point in High-Mobility Multilayer Epitaxial Graphene. *Physical Review Letters*. 2008, vol. 101, no. 26. DOI: 10.1103/PhysRevLett.101.267601.

[28] STUART, B. *Infrared spectroscopy: fundamentals and applications*. Hoboken, NJ: J. Wiley, 2004. ISBN 0-470-85427-8.

[29] HOLLAS, J. M. Basic Atomic and Molecular Spectroscopy. The Royal Society of Chemistry, 2002. ISBN 978-0-85404-667-6.

[30] COLTHUP, N. B., DALY, L.H., WIBERLEY, S. E. *Introduction to infrared and Raman spectroscopy.* Third edition. San Diego: Academic Press, 1990. ISBN 978-0-12-182554-6.

[31] JOOS, G. *Theoretical Physics.* London and Glasgow: Blackie and Son Limited, 1951. ISBN: 978-0216874046.

[32] FRITZSCHE, H. and PHILLIPS, M. "electromagnetic radiation". Encyclopedia Britannica, [online]. [cit. 2023-04-08], Available from: https://www.britannica.com/science/electromagnetic-radiation.

[33] The Nobel Prize in Physics 1918. NobelPrize.org. [online]. [cit. 2023-04-08]. Available from: https://www.nobelprize.org/prizes/physics/1918/summary/.

[34] OZAKI, Y. Infrared Spectroscopy—Mid-infrared, Near-infrared, and Far-infrared/Terahertz Spectroscopy,*Analytical Sciences*, 2021, vol. 37, no. 9, pp. 1193-1212. DOI: 10.2116/analsci.20R008.

[35] LEE, Y.-S., *Principle of Terahertz Science and Technology.* Springer, New York, 2009. ISBN: 978-0-387-09540-0.

[36] DEXHEIMER, S. L. *Terahertz Spectroscopy: Principles and Applications.* CRC Press, Boca Raton, 2008. ISBN: 978-0849375255.

[37] MANTSCH, H. H. and Naumann, D. Terahertz spectroscopy: The renaissance of far infrared spectroscopy. *Journal of Molecular Structure*. 2010, vol. 964, no. 1-3, pp. 1-4. DOI: 10.1016/j.molstruc.2009.12.022.

[38] GRIFFITH, D. W. T., JAMIE, I. M., KAWAGUCHI, K. Astronomical Vibrational Spectroscopy. In: CHALMERS, J. M. and GRIFFITHS, P. R. (Eds.) *Handbook of Vibrational Spectroscopy*, Vol. 4, Wiley, Chichester, UK, 2002, pp. 2803–2822. ISBN: 978-0471988472.

[39] FOX, M. *Optical properties of solids*. 2nd ed. Oxford: Oxford University Press, 2010. ISBN 9780199573370.

[40] HERLACH, F., MIURA, N. (n.d.). *High Magnetic Fields*. World Scientific Publishing Company. 2006. DOI: 10.1142/4764.

[41] DEW-HUGHES, D. The critical current of superconductors: an historical review. *Low Temperature Physics*. 2001, vol. 27, no. 9, pp. 713–722. DOI: 10.1063/1.1401180.

[42] SMIRNOV, A. I., SMIRNOVA, T. I., MACARTHUR, R. L., GOOD, J. A., HALL, R. Cryogen-free superconducting magnet system for multifrequency electron paramagnetic resonance up to 12.1T. *Review of Scientific Instruments*. 2006, vol. 77, no. 035108. DOI:10.1063/1.2182571.

[43] HIROSE, R., HAYASHI, S., SHIBUTANI, K. *Cryogen-free Superconducting Magnet*. KOBELCO TECHNOLOGY REVIEW NO. 27 NOV. 2007. Available from: https://www.kobelco.co.jp/english/ktr/pdf/ktr_27/018-022.pdf.

[44] AWAJI, S., WATANABE, K., OGURO, H., HANAI, S., MIYAZAKI, H., TAKAHASHI, M., IOKA, S., SUGIMOTO, M., TSUBOUCHI, H., FUJITA, S., DAIBO, M., IIJIMA, Y., KUMAKURA, H. New 25 T cryogen-free superconducting magnet project at Tohoku University. *IEEE transactions on applied superconductivity*. 2013, vol. 24, no. 3, pp. 1-5. DOI: 10.1109/TASC.2013.2292367.

[45] PADILLA, W. J., LI, Z. Q., BURCH, K. S., LEE, Y. S., MIKOLAITIS, K. J., BASOV, D. N. Broadband multi-interferometer spectroscopy in high magnetic fields: From THz to visible. *Review of Scientific Instruments*. 2004, vol. 75, no. 11, pp. 4710-4717. DOI: 10.1063/1.1805252.

[46] DRESSELHAUS, G., KIP, A. F., AND KITTEL, C. Observation of Cyclotron Resonance in Germanium Crystals. *Physical Review*. 1953, vol. 92, iss. 3, pp. 827–827. DOI: 10.1103/physrev.92.827.

[47] LAX, B., ZEIGER, H. J., DEXTER, R. N., AND ROSENBLUM, E. S. Directional Properties of the Cyclotron Resonance in Germanium. *Physical Review.* 1954, vol. 93, iss. 6, pp. 1418–1420. DOI: 10.1103/physrev.93.1418.

[48] JOHNSON, F. M., AND NETHERCOT, A. H. Antiferromagnetic Resonance in MnF_2. *Physical Review.* 1956, vol. 104, iss. 3, pp. 847–848. DOI: 10.1103/physrev.104.847.

[49] RICHARDS, P. L., CAUGHEY, W. S., EBERSPAECHER, H., FEHER, G., AND MALLEY, M. Determination of the Zero-Field Splitting of Fe3+ in Several Hemin Compounds. *Journal of Chemical Physics.* 1967, vol. 47, iss. 3, pp. 1187–1188. DOI: 10.1063/1.1712038.

[50] WANNER, M., DOEZEMA, R. E., AND STROM, U. Far-infrared surface-Landau-level spectroscopy in Bi. *Physical Review B.* 1975, vol. 12, iss. 8, pp. 2883–2892. DOI: 10.1103/physrevb.12.2883.

[51] DOEZEMA, R. E., DATARS, W. R., SCHABER, H., AND VAN SCHYNDEL, A. Far-infrared magnetospectroscopy of the Landau-level structure in graphite. *Physical Review B.* 1979, vol. 19, iss: 8, pp. 4224–4230. DOI: 10.1103/physrevb.19.4224.

[52] MOHELSKÝ, I., DUBROKA, A., WYZULA, J., SLOBODENIUK, A., MARTINEZ, G., KRUPKO, Y., PIOT, B. A., CAHA, O., HUMLÍČEK, J., BAUER, G., SPRINGHOLZ, G., ORLITA, M. Landau level spectroscopy of Bi_2Se_3. *Physical Review B.* 2020, vol. 102, no. 8, pp. 1-11. DOI: 10.1103/PhysRevB.102.085201.

[53] TIKUIŠIS, K. K., WYZULA, J., OHNOUTEK, L., CEJPEK, P., UHLÍŘOVÁ, K., HAKL, M., FAUGERAS, C., VÝBORNÝ, K., ISHIDA, A., VEIS, M., ORLITA, M. Landau level spectroscopy of the PbSnSe topological crystalline insulator, *Physical Review B.* 2021, vol. 103, no. 15. DOI: 10.1103/PhysRevB.103.155304.

[54] POLATKAN, S., GOERBIG, M. O., WYZULA, J., KEMMLER, R., MAULANA, L. Z., PIOT, B. A., CRASSEE, I., AKRAP, A., SHEKHAR, C., FELSER, C., DRESSEL, M., PRONIN, A. V., ORLITA, M. Magneto-optics of a Weyl semimetal beyond the conical band approximation: Case study of TaP, *Physical Review Letters.* 2020, vol. 124, no. 17. DOI: 10.1103/PhysRevLett.124.176402.

[55] HÜTT, F., KAMENSKYI, D., NEUBAUER, D., SHEKHAR, C., FELSER, C., DRESSEL, M., PRONIN, A. V. Terahertz transmission through TaAs single

crystals in simultaneously applied magnetic and electric fields: Possible optical signatures of the chiral anomaly in a Weyl semimetal, *Results in Physics*, 2019, vol. 15. DOI: 10.1016/j.rinp.2019.102630.

[56] LAFORGE, A. D., PADILLA, W. J., BURCH, K. S., LI, Z. Q., SCHAFGANS, A. A., SEGAWA, K., ANDO, Y., BASOV, D. N. Sum rules and interlayer infrared response of the high temperature $YBa_2Cu3_3O_y$ superconductor in an external magnetic field, *Physical Review Letters*. 2008, vol. 101, no. 9. DOI: 10.1103/PhysRevLett.101.097008.

[57] WEIL, J. A. and BOLTON, J. R. *Electron paramagnetic resonance: elementary theory and practical applications*. 2nd ed. Hoboken, N.J.: Wiley-Interscience, 2007. ISBN: 978-0471-75496-1.

[58] BOČA, R. Zero-field splitting in metal complexes. *Coordination Chemistry Reviews*. 2004, vol. 248, iss. 9–10, pp. 757–815. DOI: 10.1016/j.ccr.2004.03.001.

[59] NEHRKORN, J., VEBER, S. L., ZHUKAS, L. A., NOVIKOV, V. V., NELYUBINA, Y. V., VOLOSHIN, Y. Z., HOLLDACK, K., STOLL, S., SCHNEGG, A. Simulating Frequency-Domain Electron Paramagnetic Resonance: Bridging the Gap between Experiment and Magnetic Parameters for High-Spin Transition-Metal Ion Complexes. *The Journal of Physical Chemistry B*. 2015, vol. 119, no.43, pp. 13816-13824. DOI: 10.1021/acs.jpcb.5b04156.

[60] SESSOLI, R., GATTESCHI, D., CANESCHI, A., NOVAK, M. A. Magnetic bistability in a metal-ion cluster. *Nature*. 1993, vol. 365, no. 6442, pp. 141-143. DOI: 10.1038/365141a0.

[61] GATTESCHI, D., CORNIA, A., MANNINI, M., SESSOLI, R. Organizing and Addressing Magnetic Molecules, *Inorganic Chemistry*. 2009, vol. 48, no. 8, pp. 3408-3419.

[62] BENELLI, C. and GATTESCHI, D., *Introduction to Molecular Magnetism: From Transition Metals to Lanthanides*. Wiley-VCH, 2015.

[63] VAN SLAGEREN, J. New Directions in Electron Paramagnetic Resonance Spectroscopy on Molecular Nanomagnets. *EPR Spectroscopy*. 2011, pp. 199–234. DOI: 10.1007/128_2011_303.

[64] VAN SLAGEREN, J., VONGTRAGOOL, S., GORSHUNOV, B., MUKHIN, A., AND DRESSEL, M. Frequency-domain magnetic-resonance spectroscopic investigations of the magnetization dynamics in $Mn_{12}Ac$ single crystals. *Physical Review B*. 2009, vol. 79, iss. 22. DOI: 10.1103/physrevb.79.224406.

[65] GATTESCHI, D., SESSOLI, R., AND VILLAIN, J., *Molecular Nanomagnets*. Oxford University Press, 2006.

[66] MANNINI, M., PINEIDER, F., SAINCTAVIT, P., DANIELI, C., OTERO, E., SCIANCALEPORE, C., TALARICO, A. M., ARRIO, M.-A., CORNIA, A., GATTESCHI, D., SESSOLI, R. Magnetic memory of a single-molecule quantum magnet wired to a gold surface. *Nature Materials*. 2009, vol. 8, no. 3, pp. 194-197. DOI: 10.1038/nmat2374.

[67] PEDERSEN, K. S., ARICIU, A.-M., MCADAMS, S., WEIHE, H., BENDIX, J., TUNA, F., PILIGKOS, S. Toward Molecular 4f Single-Ion Magnet Qubits. *Journal of the American Chemical Society*. 2016, vol. 138, no. 18, pp. 5801-5804. DOI: 10.1021/jacs.6b02702.

[68] ROCHA, A. R., GARCÍA-SUÁREZ, V. M., BAILEY, S. W., LAMBERT, C. J., FERRER, J., SANVITO, S. Towards molecular spintronics. *Nature Materials*. 2005, vol. 4, no. 4, pp. 335-339. DOI: 10.1038/nmat1349.

[69] WOODRUFF, D. N., WINPENNY, R. E. P. and LAYFIELD, R. A. Lanthanide Single-Molecule Magnets. *Chemical Reviews*. 2013, vol. 113, no. 7, pp. 5110-5148. DOI: 10.1021/cr400018q.

[70] GUO, F.-S., DAY, B. M., CHEN, Y.-C., TONG, M.-L., MANSIKKAMÄKI, A., LAYFIELD, R. A. Magnetic hysteresis up to 80 kelvin in a dysprosium metallocene single-molecule magnet. *Science*. 2018, vol. 362, no. 6421, pp. 1400-1403. DOI: 10.1126/science.aav0652.

[71] VAN SLAGEREN, J. Introduction to Molecular Magnetism [online]. Physikalisches Institut, Universitt Stuttgart [cit. 2018-03-25]. Available from: http://obelix.physik.uni-bielefeld.de/~schnack/molmag/material/123.pdf.

[72] LAYFIELD, R. A. and MURUGESU, M. *Lanthanides and actinides in molecular magnetism*. Weinheim: Wiley-VCH, 2015. ISBN 978-3527335268.

[73] MISRA, S. K. *Multifrequency Electron Paramagnetic Resonance*. Weinheim, Germany: Wiley-VCH Verlag GmbH & Co., 2011. ISBN: 9783527633531.

[74] TELSER, J. EPR Interactions - Zero-field Splittings. HARRIS, R. K. a R. D. WASYLISHEN. *EMagRes*. 2017, vol 6, pp. 207-234. Chichester, UK: John Wiley. ISBN: 9780470034590.

[75] WALDMANN, O. A Criterion for the Anisotropy Barrier in Single-Molecule Magnets. *Inorganic Chemistry*. 2007, vol. 46, no. 24, pp. 10035-10037. DOI: 10.1021/ic701365t.

[76] NEESE, F. and PANTAZIS, D. A. What is not required to make a single molecule magnet. *Faraday Discuss.* 2011, vol. 148, pp. 229-238. DOI: 10.1039/C005256F.

[77] ISHIKAWA, N., SUGITA, M., ISHIKAWA, T., KOSHIHARA, S., KAIZU, Y. Lanthanide Double-Decker Complexes Functioning as Magnets at the Single-Molecular Level. *Journal of the American Chemical Society.* 2003, vol. 125, no. 29, pp. 8694-8695. DOI: 10.1021/ja029629n.

[78] NEHRKORN, J., VEBER, S. L., ZHUKAS, L. A., NOVIKOV, V. V., NELYUBINA, Y. V., VOLOSHIN, Y. Z., HOLLDACK, K., L, S., SCHNEGG, A. Determination of Large Zero-Field Splitting in High-Spin Co(I) Clathrochelates. *Inorganic Chemistry.* 2018, vol. 57, no. 24, pp. 15330-15340. DOI: 10.1021/acs.inorgchem.8b02670.

[79] KRZYSTEK, J., OZAROWSKI, A., TELSER, J. Multi-frequency, high-field EPR as a powerful tool to accurately determine zero-field splitting in high-spin transition metal coordination complexes. *Coordination Chemistry Reviews.* 2006, vol. 250, no. 17-18, pp. 2308-232. DOI: 10.1016/j.ccr.2006.03.016.

[80] SCHNEGG, A. Very-high-frequency EPR. HARRIS, R. K. a R. D. WASYLISHEN. *EMagRes.* 2017, vol 6, pp. 115-132. Chichester, UK: John Wiley. ISBN 9780470034590.

[81] KITTEL, Ch. *Introduction to solid state physics.* 2005. 8th ed. Hoboken: John Wiley. ISBN 0-471-41526-x.

[82] ORLITA, M. and POTEMSKI, M. Dirac electronic states in graphene systems: optical spectroscopy studies. *Semiconductor Science and Technology.* 2010, vol. 5, no. 6. DOI: 10.1088/0268-1242/25/6/063001.

[83] NEDOLIUK, I. *Infared magneto-optical spectroscopy of boron nitride encapsulated graphene.* 2018, GENÈVE. Available from: http://archive-ouverte.unige.ch/unige:114899. Dissertation Thesis. UNIVERSITÉ DE GENÈVE.

[84] SOJKA, A. *Development of a Terahertz Magnetic Resonance Spectrometer for Electron Spin Dynamics Investigations.* Brno, 2022. Doctoral thesis. Brno University of Technology. Central European Institute of Technology. Supervised by Ing. Petr Neugebauer, PhD.

[85] SOJKA, A., ŠEDIVÝ, M., LAGIŇ, A., GABRIŠ, A., LÁZNIČKA, T., SANTANA, V. T., LAGUTA, O., NEUGEBAUER, P. Sample Holders for Sub-THz

Electron Spin Resonance Spectroscopy, *IEEE Transactions on Instrumentation and Measurement*, vol. 71, pp. 1-12, 2022. DOI: 10.1109/TIM.2022.3164135.

[86] LAGIŇ, A. *Design of non-resonant sample holders.* Brno, 2020. Available at: https://www.vutbr.cz/studenti/zav-prace/detail/124733. Bachelor thesis. Brno University of Technology, Faculty of Mechanical Engineering, Institute of Machine and Industrial Design. Supervised by Ing. Antonín Sojka.

[87] EL FATIMY, A., *et al.* Epitaxial graphene quantum dots for high-performance terahertz bolometers. *Nature Nanotechnology*. 2016, vol. 11, no. 4, pp. 335-338. DOI: 10.1038/nnano.2015.303.

[88] EL FATIMY, A., *et al.* Ultra-broadband photodetectors based on epitaxial graphene quantum dots. *Nanophotonics*. 2018, vol. 7, no. 4, pp. 735-740. DOI: 10.1515/nanoph-2017-0100.

[89] MARIE, L. S., EL FATIMY, A., HRUBÝ, J., NEMEC, I., HUNT, J., MYERS-WARD, R., GASKILL, D. K., KRUSKOPF, M., YANG, Y., ELMQUIST, R., MARX, R., VAN SLAGEREN, J., NEUGEBAUER, P., BARBARA, P. Nanostructured graphene for nanoscale electron paramagnetic resonance spectroscopy. *Journal of Physics: Materials*. 2020, vol. 3, no. 014013. DOI: 10.1088/2515-7639/ab6af8.

[90] DRESSELHAUS, G., KIP, A. F., KITTEL, C. Cyclotron Resonance of Electrons and Holes in Silicon and Germanium Crystals. *Physical Review*. 1955, vol. 98, iss. 2, pp. 368–384. DOI: 10.1103/physrev.98.368.

[91] YU, P. Y., and CARDONA, M., *Fundamentals of Semiconductors, Graduate Texts in Physics*, 4th ed., Springer-Verlag, Berlin Heidelberg, 2010. ISBN: 978-3-642-00710-1.

[92] MIURA, N. Physics of semiconductors in high magnetic fields. Oxford: Oxford University Press. 2008. ISBN 978–0–19–851756–6.

[93] KESSLER, F. R. and METZDORF, J. CHAPTER 11 - Landau Level Spectroscopy: Interband Effects and Faraday Rotation. In: LANDWEHR, G., RASHBA, E. I.*Modern Problems in Condensed Matter Sciences*, Elsevier. 1991, vol. 27, no. 1, pp. 579-675, 1991. ISBN: 978-0444885357.

[94] VARSHNI, Y. P. Temperature dependence of the energy gap in semiconductors, *Physica*. 1967, vol. 34, no. 1, pp. 149–154. DOI: 10.1016/0031-8914(67)90062-6.

Author publications and outputs

Publications (09/2023) https://orcid.org/0000-0003-1381-7469

- **Dubnická Midlíková, J.**; Šedivý, M.; Sojka, A.; Tadeu Santana, V.; Dubroka, A.; Neugebauer, P. A Versatile Setup for FTIR Magneto-Spectroscopy *IEEE Transactions on Instrumentation and Measurement*, vol. 72, pp. 1-11, 2023. DOI: 10.1109/TIM.2023.3284943. (Impact Factor (IF)=5.33, Q1, 0 cit.)
- Malinová, N.; Juráková, J.; Brachňaková, B.; **Dubnická Midlíková, J.**; Čižmár, E.; Tadeu Santana, V.; Herchel, R.; Orlita, M.; Mohelský, I.; Moncol, J.; Neugebauer, P.; Šalitroš, I. Magnetization Slow Dynamics in Mononuclear Co(II) Field-Induced Single-Molecule Magnet. *Crystal Growth & Design*, 23, 4, 2430–2441, 2023. DOI: 10.1021/acs.cgd.2c01388. (IF=4.01, Q1, 0 cit.)
- Juráková, J.; **Dubnická Midlíková, J.**; Hrubý, J.; Kliukov, A.; Tadeu Santana, V.; Pavlik, J.; Moncoľ, J.; Čižmár, E.; Orlita, M.; Mohelský, I.; Neugebauer, P.; Gentili, D.; Cavallini, M.; Šalitroš, I. Pentacoordinate cobalt(II) single ion magnets with pendant alkyl chains: shall we go for chloride or bromide? *Inorg. Chem. Front.* 9, 1179-1194, 2022. DOI: 10.1039/D1QI01350E. (IF=7.78, Q1, 10 cit.)
- Bamberger, H.; Albold, U.; **Dubnická Midlíková, J.**; Su, C.-Y.; Deibel, N.; Hunger, D.; Hallmen, P. P.; Neugebauer, P.; Beerhues, J.; Demeshko, S.; Meyer, F.; Sarkar, B.; van Slageren, J. Iron(II), Cobalt(II), and Nickel(II) Complexes of Bis(sulfonamido)benzenes: Redox Properties, Large Zero-Field Splittings, and Single-Ion Magnets. *Inorg. Chem.* 60, 2953–2963, 2021. DOI: 10.1021/acs.inorgchem.0c02949. (IF=5.44, Q1, 12 cit.)

Internships

- 10/2021 – One-month research stay at the **Department of Physics, Georgetown University** in Washington DC, USA, group of Prof. Paola Barbara. Topic: *Transport measurements on graphene bolometer devices.*
- 04/2019 – One-month research stay at **Grenoble High Magnetic Field Laboratory (GHMFL)** in France, sponsored by CEITEC mobility contribution 2018. French National Center for Scientific Research (CNRS), group of Dr. Milan Orlita. Topic: *FTIR measurements with graphene bolometer devices.*
- 04/2018 – Short-Term Scientific Mission in Molecular Spintronics (MOLSPIN) in Germany sponsored by COST Action scholarship. **Institute of Physical Chemistry at University of Stuttgart**, group of prof. Joris van Slageren, Topic: *Coupling of the far-infrared spectrometer to a superconductive magnet and magneto-optical measurements in far-infrared region.*

- 04/2017 – Research stay at **Grenoble High Magnetic Field Laboratory (GHMFL)** in France, sponsored by University of Stuttgart. French National Center for Scientific Research (CNRS), group of Dr. Milan Orlita. Topic: *Infrared magneto-spectroscopy of mononuclear Co-complexes.*
- 02-07/2017 – Erasmus+ scholarship project in Germany, **Institute of Physical Chemistry at University of Stuttgart**, group of prof. J. van Slageren. Topic: *Coupling of the FIR spectrometer to a 17 T superconducting magnet.*

Conferences

- 09/2022 – Alpine Conference on Magnetic Resonance in Solids 2022, Chamonix-Mont-Blanc, France – **Oral contribution** (round table presentation)
- 06/2021 – 17th International Conference on Molecule Based Magnets (ICMM2021), Manchester, United Kingdom (online) – **Poster contribution, award**
- 09/2019 – 11th European Federation of EPR groups (EFEPR) Conference Bratislava 2019, Slovakia – **Poster contribution**
- 07/2018 – International Conference on Nanoscience+Technology 2018 (ICN+T 2018) Brno, Czech Republic – **Poster contribution**

Summer Schools, Workshops, Retreats

- 09/2021 – CEITEC PhD Retreat 2021, Brno, Czech Republic (online) – **Oral contribution** (flash talk)
- 11/2019 – 8th School of the European Federation of EPR groups on Advanced EPR (EFEPR School 2019) Brno, Czech Republic – **Poster contribution**
- 06/2019 – CEITEC PhD Joint Retreat in Hotel Luna, Czech Republic – **Oral contribution** (flash talk)
- 06/2019 – Plasmon Enhanced Terahertz Electron Paramagnetic Resonance (PETER) Project - International Workshop, Hirschegg, Austria
- 06/2019 – 2nd MOTeS Retreat 2019, Masłońskie, Poland – **Oral contribution**
- 11/2018 – 3rd CEITEC NANO User meeting, Brno – **Poster contribution**
- 10/2018 – Plasmon Enhanced Terahertz Electron Paramagnetic Resonance (PETER) Summer School in Brno, Czech Republic – **Oral contribution**
- 09/2018 – V.International School for Young Scientists. Magnetic Resonance and Magnetic Phenomena in Chemical and Biological Physics, St. Petersburg, Russia – **Poster and Oral contribution** (flash talk)
- 06/2019 – 1st MOTeS Retreat 2018 in Vyhne, Slovakia – **Oral contribution**

Projects

- 12/2019 – **Inter-Excellence USA-CZ 2019** (LTAUSA19060) – member of the international solving team.

- 03/2019 – **Internal junior grant project** within the CEITEC BUT 2019 – principal investigator.
- 01/2019 – **Brno PhD Talent 2018** project – principal investigator.

Awards

- 06/2021 – **Outstanding Poster Presentation Prize** at ICMM2021 conference in Manchester (UK) awarded by RSC Inorganic Chemistry Frontiers.
- 12/2018 – **Brno PhD Talent 2018** Scholarship – awarded by JCMM Brno.
- 10/2018 – **Edwards Award** 2018 – 4th place for my master's thesis.

Products/Functional Specimens

- Movable Table for FTIR Magneto-Spectroscopic Setup
- FTIR Magneto-Spectroscopic Optical Coupling
- FTIR Magneto-Spectroscopic Transmission Probe for External Detectors
- FTIR Magneto-Spectroscopic Transmission Probe for Internal Detectors
- FTIR Magneto-Spectroscopic Transmission Probe with Chipset Holder

Teaching

- 09-12/2020 (winter semester) – **Principles of Measurement (1ZM)** in Engineering at Faculty of Mechanical Engineering, Brno University of Technology.
- 09-12/2019 (winter semester) – **Principles of Measurement (1ZM)** in Engineering at Faculty of Mechanical Engineering, Brno University of Technology.
- 02-05/2019 (summer semester) – **Physics (BF)** at Faculty of Mechanical Engineering, Brno University of Technology.
- 09-12/2018 (winter semester) – **Principles of Measurement (1ZM)** in Engineering at Faculty of Mechanical Engineering, Brno University of Technology.

Voluntary Activitites

- 11/2019 – **8th School of the European Federation of EPR groups on Advanced EPR 2019** in Brno, Czech Republic, co-organizer.
- 09/2019 – **Researcher's Night 2019** at CEITEC BUT, performing experiments for public.
- 09/2018 – **Researcher's Night 2018** at CEITEC BUT, performing experiments for public.
- 07/2018 – **International Conference on Nanoscience+Technology 2018** (ICN+T 2018) Brno, Czech Republic, navigator of the conference participants.